1 **Gle1 is required for tRNA to stimulate Dbp5 ATPase activity *in vitro* and to promote Dbp5**
2 **mediated tRNA export *in vivo*.**
3

4 Arvind Arul Nambi Rajan[1], Ryuta Asada[2] and Ben Montpetit[1,2,#]

5 [1] Biochemistry, Molecular, Cellular and Developmental Biology Graduate Group, University of California
6 Davis, Davis, CA, USA

7 [2] Department of Viticulture and Enology, University of California Davis, Davis, CA, USA

8 [#] Correspondence should be sent to: Ben Montpetit (benmontpetit@ucdavis.edu)

9

10 Keywords: DBP5, DDX19, GLE1, MEX67, mRNA export, tRNA export

ABSTRACT

Cells must maintain a pool of processed and charged transfer RNAs (tRNA) to sustain translation capacity and efficiency. Numerous parallel pathways support the processing and directional movement of tRNA in and out of the nucleus to meet this cellular demand. Recently, several proteins known to control messenger RNA (mRNA) transport were implicated in tRNA export. The DEAD-box Protein 5, Dbp5, is one such example. In this study, genetic and molecular evidence demonstrates that Dbp5 functions parallel to the canonical tRNA export factor Los1. *In vivo* co-immunoprecipitation data further shows Dbp5 is recruited to tRNA independent of Los1, Msn5 (another tRNA export factor), or Mex67 (mRNA export adaptor), which contrasts with Dbp5 recruitment to mRNA that is abolished upon loss of Mex67 function. However, as with mRNA export, overexpression of Dbp5 dominant-negative mutants indicates a functional ATPase cycle and that binding of Dbp5 to Gle1 is required by Dbp5 to direct tRNA export. Biochemical characterization of the Dbp5 catalytic cycle demonstrates the direct interaction of Dbp5 with tRNA (or double stranded RNA) does not activate Dbp5 ATPase activity, rather tRNA acts synergistically with Gle1 to fully activate Dbp5. These data suggest a model where Dbp5 directly binds tRNA to mediate export, which is spatially regulated via Dbp5 ATPase activation at nuclear pore complexes by Gle1.

27 **INTRODUCTION**

28 Key to the production of proteins is the delivery of amino acids to ribosomes by transfer RNAs
29 (tRNAs). Precursor tRNAs (pre-tRNAs) are first transcribed by RNA Polymerase III with a 5´ leader and
30 a 3´ trailer sequence (Guerrier-Takada, Gardiner et al. 1983, Cook, Fukuhara et al. 2009, Skowronek,
31 Grzechnik et al. 2014, Harris 2016, Graczyk, Ciesla et al. 2018). To function in translation, pre-tRNAs
32 must be end matured and modified, spliced, amino-acylated and exported from the nucleus in eukaryotes.
33 Importantly, it has come to be appreciated that these steps in tRNA processing are not necessarily
34 sequential (Trotta, Miao et al. 1997, Yoshihisa, Yunoki-Esaki et al. 2003, Yoshihisa, Ohshima et al. 2007,
35 Wu and Hopper 2014, Hopper and Huang 2015, Wu, Bao et al. 2015, Phizicky and Hopper 2023). For
36 example, in the budding yeast *Saccharomyces cerevisiae,* intron-containing tRNAs are spliced in the
37 cytoplasm on the mitochondrial surface by the tRNA Splicing Endonuclease (SEN) complex following
38 nuclear export (Yoshihisa, Yunoki-Esaki et al. 2003, Yoshihisa, Ohshima et al. 2007, Skowronek,
39 Grzechnik et al. 2014, Wan and Hopper 2018). Furthermore, cytoplasmic tRNAs can be reimported to
40 the nucleus through retrograde transport to allow tRNAs to undergo further modification and quality
41 control which is also used to repress translation during conditions of stress (Murthi, Shaheen et al. 2010,
42 Hopper and Huang 2015, Nostramo and Hopper 2020). As tRNAs cycle between the nucleus and
43 cytoplasm, they undergo various chemical modifications that are also spatially regulated (Phizicky and
44 Hopper 2023). The proper processing and modification of tRNAs through this complex regulatory network
45 dictates proper folding of pre-tRNAs and recognition by appropriate tRNA binding proteins that control
46 subsequent steps in the tRNA life cycle.

47 In the context of nuclear export, end maturation and amino-acylation are required for recognition
48 by the tRNA Exportin Los1/Exportin-t and Msn5 respectively (Huang and Hopper 2015, Chatterjee,
49 Majumder et al. 2017, Nostramo and Hopper 2020, Chatterjee, Marshall et al. 2022). Although Los1 and
50 Msn5 are the best characterized tRNA export factors, both are non-essential and can be deleted in
51 combination (Takano, Endo et al. 2005, Murthi, Shaheen et al. 2010). Given the essential nature of tRNA

52 export, this has prompted several studies, including a comprehensive screen of nearly all annotated
53 genes in *S. cerevisiae,* to identify additional factors responsible for regulating nucleocytoplasmic
54 dynamics of tRNA localization and processing (Feng and Hopper 2002, Steiner-Mosonyi, Leslie et al.
55 2003, Eswara, McGuire et al. 2009, Huang and Hopper 2015, Wu, Bao et al. 2015, Chatterjee, Majumder
56 et al. 2017, Nostramo and Hopper 2020, Chatterjee, Marshall et al. 2022). These studies have elucidated
57 functional roles of the karyopherin Crm1 and mobile nucleoporin Mex67 in regulating tRNA
58 nucleocytoplasmic dynamics (Chatterjee, Majumder et al. 2017, Derrer, Mancini et al. 2019, Nostramo
59 and Hopper 2020, Chatterjee, Marshall et al. 2022). Both factors have previously been shown to function
60 in messenger RNA (mRNA) export (Hodge, Colot et al. 1999, Takemura, Inoue et al. 2004, Lund and
61 Guthrie 2005, Derrer, Mancini et al. 2019), with Mex67 serving an essential role in the process (Hodge,
62 Colot et al. 1999, Lund and Guthrie 2005, Adams and Wente 2020). In tRNA export, it is thought that
63 Crm1 and Mex67 both function parallel to Los1 to support export of pre-tRNA and re-export of spliced
64 tRNA that have undergone retrograde transport (Chatterjee, Majumder et al. 2017, Nostramo and Hopper
65 2020, Chatterjee, Marshall et al. 2022). Moreover, recent reports suggest subspecies specialization and
66 family preferences for tRNA cargo, with Mex67 serving a unique function in the premature export of pre-
67 tRNAs that have not completed 5´ end processing (Chatterjee, Marshall et al. 2022).

68 While non-coding RNA (ncRNA) and mRNA export pathways have long been hypothesized to be
69 regulated by independent processes, recent studies indicate the participation of numerous mRNA export
70 factors in regulation of diverse ncRNAs (Yao, Roser et al. 2007, Yao, Lutzmann et al. 2008, Faza, Chang
71 et al. 2012, Bai, Moore et al. 2013, Wu, Becker et al. 2014, Becker, Hirsch et al. 2019, Vasianovich, Bajon
72 et al. 2020). In addition to tRNA and mRNA, both Mex67 and Crm1 have functions in pre-snRNA, pre-
73 ribosomal subunit, and *TLC1* (telomerase) export (Yao, Roser et al. 2007, Faza, Chang et al. 2012, Bai,
74 Moore et al. 2013, Wu, Becker et al. 2014, Becker, Hirsch et al. 2019, Vasianovich, Bajon et al. 2020).
75 Similarly, in addition to Mex67 and Crm1, the DEAD-box Protein 5 (Dbp5) has also been implicated in
76 each of these RNA export pathways, including tRNA export (Wu, Becker et al. 2014, Neumann, Wu et

77 al. 2016, Mikhailova, Shuvalova et al. 2017, Becker, Hirsch et al. 2019, Lari, Arul Nambi Rajan et al.
78 2019). Dbp5 is most well known as an RNA-stimulated ATPase that is spatially regulated by the
79 nucleoporins Nup159 and Gle1 with the small molecule inositol hexakisphosphate ($InsP_6$) at the
80 cytoplasmic face of the nuclear pore complex (NPC) to promote the directional export of mRNA (Snay-
81 Hodge, Colot et al. 1998, Tseng, Weaver et al. 1998, Hodge, Colot et al. 1999, Schmitt, von Kobbe et al.
82 1999, Strahm, Fahrenkrog et al. 1999, Zhao, Jin et al. 2002, Weirich, Erzberger et al. 2004, Lund and
83 Guthrie 2005, Alcazar-Roman, Tran et al. 2006, Weirich, Erzberger et al. 2006, Tran, Zhou et al. 2007,
84 Dossani, Weirich et al. 2009, Fan, Cheng et al. 2009, von Moeller, Basquin et al. 2009, Hodge, Tran et
85 al. 2011, Montpetit, Thomsen et al. 2011, Noble, Tran et al. 2011, Kaminski, Siebrasse et al. 2013, Wong,
86 Cao et al. 2016, Adams, Mason et al. 2017, Wong, Gray et al. 2018, Adams and Wente 2020). In addition
87 to these export roles, Dbp5 also shuttles between the nucleus and cytoplasm with reported roles in
88 transcription, R-loop metabolism, and translation (Hodge, Colot et al. 1999, Estruch and Cole 2003,
89 Gross, Siepmann et al. 2007, Scarcelli, Viggiano et al. 2008, Tieg and Krebber 2013, Mikhailova,
90 Shuvalova et al. 2017, Lari, Arul Nambi Rajan et al. 2019, Beissel, Grosse et al. 2020). Notably, Nup159
91 and Gle1 mutants also alter tRNA export (Lari, Arul Nambi Rajan et al. 2019), suggesting the mRNA
92 export pathway as a whole (e.g., Mex67, Dbp5, Gle1/ $InsP_6$, Nup159) may support tRNA export.
93 However, a mechanistic understanding of how Dbp5 supports these diverse functions and whether they
94 are regulated by similar co-factors and enzymatic activity is largely not understood.

95 A recent mutagenesis screen within our research group identified mutants that alter the
96 nucleocytoplasmic shuttling dynamics of Dbp5 (Lari, Arul Nambi Rajan et al. 2019). Mutations were
97 identified (e.g., $dbp5^{L12A}$) that disrupt a nuclear export sequence (NES) recognized by Crm1 to promote
98 Dbp5 transport out of the nucleus. In contrast, another mutant, $dbp5^{R423A}$, was found to be impaired in
99 nuclear import from the cytoplasm. Importantly, neither of these mutations disrupt the essential mRNA
100 export functions of Dbp5; however, limited nuclear access of $dbp5^{R423A}$ induced tRNA export defects
101 suggesting a potentially novel role for nuclear Dbp5 in tRNA export. In support of this hypothesis, a

102 physical interaction between Dbp5 and tRNA was also characterized, which was elevated upon nuclear
103 accumulation of Dbp5 in a *dbp5*^{L12A} mutant (Lari, Arul Nambi Rajan et al. 2019).

104 In this study, genetic and biochemical characterization of Dbp5 mediated tRNA export was
105 performed. The data show that Dbp5 is recruited to pre-tRNA independent of Los1, Msn5, and Mex67,
106 positioning the DEAD-box protein function parallel to the primary Los1 mediated pre-tRNA export
107 pathway. In contrast to single stranded RNA substrates (e.g., mRNA), this study further demonstrates an
108 interaction of Dbp5 with tRNA and double stranded RNA (dsRNA) that leads to robust ATPase activation
109 only in the presence of Gle1/ $InsP_6$. These findings, together with previous research (Lari, Arul Nambi
110 Rajan et al. 2019), suggest that Dbp5 engages tRNA within the nucleus in a manner distinct from mRNA,
111 and requires Gle1/ $InsP_6$ to mediate RNA stimulated ATPase activation of Dbp5 to promote export.

112

113 **RESULTS**

114 ***Dbp5 functions parallel to Los1 in pre-tRNA export***

115 Previous studies have placed the mRNA export factor Mex67, a proposed target of Dbp5
116 regulation in mRNA export (Lund and Guthrie 2005, Adams and Wente 2020), in a pathway parallel to
117 Los1 regulated pre-tRNA nucleo-cytoplasmic shuttling (Chatterjee, Majumder et al. 2017). To investigate
118 the relationship between Dbp5 and Los1, it was first determined if the subcellular distribution of either
119 protein was dependent on the activity of the other. In a *los1Δ,* the NPC localization of GFP-Dbp5 was not
120 altered (Figure 1A). Similarly, when a Dbp5 loss of function was induced using Auxin Induced
121 Degradation (AID) (Nishimura, Fukagawa et al. 2009), Los1-GFP localization remained unchanged
122 (Figure 1B) while mRNA export defects were detected (Figure 1C), confirming depletion of Dbp5 to a
123 level sufficient to disrupt mRNA export. To test the genetic and phenotypic relationship of Los1 and Dbp5,
124 a *los1Δ* was combined with the previously identified Dbp5 shuttling mutants (i.e., *dbp5*^{L12A} and *dbp5*^{R423}).
125 Like a *mex67-5/los1Δ* strain (Chatterjee, Majumder et al. 2017), double mutants of *los1Δ* with *dbp5*^{L12A}
126 (increased in the nucleus) or *dbp5*^{R423} (depleted from the nucleus) exhibited no growth defects (Figure

127 1D). In contrast, by tRNA FISH using a probe specific to the $tRNA^{Ile}_{UAU}$ intron (SRIM03), the *los1Δ*
128 *dbp5*^{R423A} double mutant exhibited significantly stronger nuclear accumulation of pre-tRNA as compared
129 to single mutants or control after a 4-hour incubation at 37°C (Figure 1E/F). Notably, elevating nuclear
130 pools of Dbp5 by combining *dbp5*^{L12A} with *los1Δ* did not alter the pre-tRNA export defects observed in
131 *los1Δ* strains, indicating that excess nuclear Dbp5 is not sufficient to suppress the *los1Δ* phenotype. To
132 complement the FISH data, Northern blotting analyses were conducted to assess tRNA processing in
133 the double mutants. Intron-containing pre-tRNAs are transcribed with 5´ leader and 3´ trailer sequences
134 to generate precursor molecules (P) that are end-processed in the nucleus to generate intron-containing
135 intermediates (I) that can be detected by Northern blotting (Wu, Bao et al. 2015). When nuclear export of
136 the end-processed pre-tRNA is disrupted a change in the precursor (P) to intron-containing intermediate
137 (I) ratio is observed (Wu, Huang et al. 2013, Wu, Bao et al. 2015, Chatterjee, Majumder et al. 2017). As
138 such, I/P ratios were measured in the *los1Δ/dbp5* double mutants. In line with the increased nuclear
139 localization of pre-tRNAs observed by FISH, an additive defect in pre-tRNA processing was observed
140 when *los1Δ* was combined *dbp5*^{R423A} (~2-fold increase in the I/P ratio relative to *los1Δ* alone, Figure
141 1G/H). These FISH and Northern blotting data mirror phenotypes previously reported for mutants of
142 Mex67 in relation to Los1 (Chatterjee, Marshall et al. 2022), and ultimately place Dbp5 in a tRNA export
143 pathway that has functions parallel to Los1.

144

145 ***Known tRNA export factors do not recruit Dbp5 to pre-tRNAs in vivo***

146 Dbp5, like other DEAD-box proteins, has been reported to bind nucleic acids through sequence
147 independent interactions with the phosphate backbone (Andersen, Ballut et al. 2006, Bono, Ebert et al.
148 2006, Sengoku, Nureki et al. 2006, Montpetit, Thomsen et al. 2011). For other helicases of the SF2 family,
149 specificity in RNA substrates is conferred by adaptor proteins (Lund and Guthrie 2005, Jankowsky 2011,
150 Thoms, Thomson et al. 2015). For this reason, it was investigated whether known tRNA export factors
151 mediate recruitment of Dbp5 to pre-tRNA substrates. To do so, RNA immunoprecipitation (RIP)

152 experiments were performed with protein-A (prA) tagged Dbp5, integrated at its endogenous locus and
153 present as the sole copy of the gene, in strains where tRNA export factors were deleted. Co-
154 immunoprecipitated RNAs were analyzed by RT-qPCR with primers specific to un-spliced intron-
155 containing pre-tRNA$^{Ile}_{UAU.}$ The abundance of the pre-tRNA$^{Ile}_{UAU}$ target in each IP was normalized to the
156 abundance of the target in the corresponding input sample to control for changes in gene expression.
157 Relative enrichment of the target RNA was then compared to the background signal obtained from RNA
158 IPs in a common untagged control. In a *los1Δ* strain, a ~2-fold reduction in the relative amount of pre-
159 tRNA co-immunoprecipitated with Dbp5 (~9.5-fold enrichment in WT to ~4.5-fold in *los1Δ*) was observed,
160 but the deletion failed to abolish the Dbp5 pre-tRNA *in vivo* interaction (Figure 2A). Loss of Msn5, which
161 does not have a published role in the export of intron-containing pre-tRNAs (Huang and Hopper 2015),
162 did not cause a significant change in Dbp5 pre-tRNA interactions by RNA IP. These results are consistent
163 with the additive tRNA export defects observed in *los1Δ dbp5*^{R423A} double mutants reported in Figure 1
164 and support the hypothesis that Dbp5 functions in tRNA export parallel to Los1.

165 In mRNA export, Mex67 is a proposed target of Dbp5 activity to promote directional nuclear export
166 (Adams and Wente 2020). Since neither of the non-essential tRNA export factors abolished Dbp5-tRNA
167 interaction when deleted, it was tested if Mex67 has a role in recruiting Dbp5 to tRNA. An Anchors Away
168 approach was used to rapidly re-localize Mex67 to the cytoplasmic peroxisomal anchor (Pex25-FKBP12)
169 in an inducible manner dependent on the addition of rapamycin (Haruki, Nishikawa et al. 2008). The
170 resulting strains were sensitive to rapamycin, causing nuclear mRNA accumulation by dT FISH within 15
171 minutes of addition (Fig 2D). This timing is consistent with a previous report employing Mex67 Anchors
172 Away (Mex67-AA) (Tudek, Schmid et al. 2018). PrA-Dbp5 was integrated at its endogenous locus in
173 these strains and RNA-IP experiments were performed before and after rapamycin addition as described
174 above. Under these conditions of Mex67-AA re-localization, no significant change in the Dbp5-tRNA$^{Ile}_{UAU}$
175 interaction was observed (median of ~8.8-fold enrichment before addition of rapamycin and ~8.2-fold
176 after, Figure 2B). Importantly, consistent with the function of Mex67 mRNA export (Snay-Hodge, Colot et

177 al. 1998, Tseng, Weaver et al. 1998, Schmitt, von Kobbe et al. 1999, Strahm, Fahrenkrog et al. 1999,
178 Weirich, Erzberger et al. 2004, Lund and Guthrie 2005, Tran, Zhou et al. 2007, Dossani, Weirich et al.
179 2009, von Moeller, Basquin et al. 2009, Adams and Wente 2020), the nuclear retention of mRNAs via
180 Mex67-AA resulted in strongly reduced binding of Dbp5 to the *FBA1* mRNA (from a median of ~8 fold
181 enrichment above background before addition of rapamycin to no enrichment after, Figure 2C). Together,
182 these RNA IP experiments suggest that Dbp5 binds to tRNAs independent of known tRNA export proteins
183 and does so in a manner that is distinct from mRNA.

184

185 ***The Dbp5 ATPase cycle supports tRNA export in vivo***

186 In mRNA export, RNA binding, Gle1 activation, and ATP hydrolysis by Dbp5 are all critical for
187 directional transport (Hodge, Tran et al. 2011, Noble, Tran et al. 2011). The *dbp5*^{R426Q} and *dbp5*^{R369G}
188 mutants have previously been shown to exhibit deficient RNA binding (<5% of WT), ATPase activity
189 (~10% and 60% of WT, respectively) and have a dominant-negative effects on mRNA export status when
190 overexpressed (Hodge, Tran et al. 2011, Noble, Tran et al. 2011). Additionally, it has been shown that
191 *dbp5*^{R369G} has elevated Gle1 affinity and effectively competes with WT Dbp5 for Gle1 binding (Hodge,
192 Tran et al. 2011). In contrast, *dbp5*^{E240Q} is an ATP hydrolysis mutant that is competent to bind RNA, as it
193 is biased to the ATP bound state, but is recessive lethal showing no mRNA export defect when
194 overexpressed in the context of endogenously expressed WT Dbp5 (Hodge, Tran et al. 2011). Unlike the
195 impact of these mutants on mRNA export, it has been reported that the ability of Dbp5 to complete ATP
196 hydrolysis (but not RNA binding) is dispensable for pre-ribosomal subunit export, as is Gle1 (Neumann,
197 Wu et al. 2016).

198 Based on the observation that Gle1 functions to support tRNA export (Lari, Arul Nambi Rajan et
199 al. 2019), these Dbp5 mutants deficient in ATPase activity or altered Gle1 binding were tested for their
200 influence on tRNA export to infer if tRNA export is more similar to mRNA or pre-ribosomal subunit export.
201 To individually express these lethal mutants and the wildtype control, *DBP5*, *dbp5*^{R426Q}, *dbp5*^{R369G}, or

202 *dbp5*^{E240Q} were integrated at the *URA3* locus under regulation of the inducible pGAL promoter. Protein
203 expression was induced for 6 hours by shifting cells from raffinose to galactose containing media.
204 Importantly, induction was followed by 1 hour of growth in glucose to halt expression and relieve potential
205 changes in tRNA export induced by a change in the primary carbon source. Using this approach, all
206 proteins were expressed as indicated by western blotting (Figure 3A) and showed the previously reported
207 impact on mRNA export (Figure 3B). Northern blotting targeting $tRNA^{Ile}_{UAU}$ revealed both *dbp5*^{R426Q} and
208 *dbp5*^{R369G}*,* but not *dbp5*^{E240Q}*,* showed an accumulation of intron-containing precursor $tRNA^{Ile}_{UAU}$ as
209 compared to over expression of wildtype Dbp5 (I/P ratio of 1.97 +/- 0.06 vs 1.93 +/- 0.31 vs 1.32 +/- 0.41,
210 respectively) (Figure 3C/D). These phenotypes differ from the reported impacts on pre-ribosomal subunit
211 transport, indicating Dbp5 functions differently in these non-coding RNA export pathways. Furthermore,
212 these data indicate that both the ATPase cycle and regulation of Dbp5 by Gle1 are central to the function
213 of Dbp5 in tRNA export, as each activity is in mRNA export.

214

215 ***Dbp5 ATPase activity in the presence of tRNA is Gle1-dependent***

216 Given the impact of *dbp5*^{R426Q} and *dbp5*^{R369G} overexpression on tRNA export *in vivo*, the Dbp5
217 ATPase cycle and role of Gle1 in the context of tRNA was further investigated *in vitro*. Previous studies
218 have characterized Dbp5 binding to single stranded RNA (ssRNA) substrates and demonstrated Dbp5
219 binding to ssRNA is linked to the nucleotide state of the enzyme, with the highest affinity for ssRNA
220 occurring when Dbp5 is ATP bound (Weirich, Erzberger et al. 2006, Montpetit, Thomsen et al. 2011, Arul
221 Nambi Rajan and Montpetit 2021). Following ssRNA binding, hydrolysis of ATP to ADP results in a
222 reduction in the affinity of Dbp5 for the ssRNA substrate (Weirich, Erzberger et al. 2006). While there has
223 been extensive characterization of the structural and biochemical details of Dbp5, ssRNA, and co-
224 regulators (Wong, Gray et al. 2018, Mason and Wente 2020, Gray, Cao et al. 2022), no such
225 understanding exists for Dbp5 engaging highly structured RNA substrates like tRNA. As such, it was first
226 tested if recombinant full length Dbp5 could bind commercially available yeast mixed tRNAs or the yeast

227 Phenylalanine tRNA (both substrates that have been used in previous biochemical and structural studies
228 (Shi and Moore 2000, Yao, Roser et al. 2007)). To test whether Dbp5 can form complexes with tRNA *in*
229 *vitro,* electrophoretic mobility shift assays (EMSA) were performed in the presence of different nucleotide
230 states and tRNA substrates. Consistent with published observations of complex formation between Dbp5
231 and ssRNA (Weirich, Erzberger et al. 2006, Montpetit, Thomsen et al. 2011), Dbp5 generated band shifts
232 for both mixed tRNA substrates and Phe tRNA in the presence of the ATP state analog ADP•BeF_3 (Figure
233 4A). In the presence of ATP or ADP, or with no nucleotide, Dbp5 failed to form a similar band shift, which
234 exactly parallels reported interactions between Dbp5 and ssRNA in these nucleotide states (Weirich,
235 Erzberger et al. 2006, Montpetit, Thomsen et al. 2011).

236 To further estimate an affinity for tRNA, both the Phenylalanine tRNA and yeast mixed tRNAs
237 were used in EMSA experiments with varying concentrations of Dbp5 (and fixed concentrations of
238 ADP•BeF_3 and tRNA). From quantification of the EMSAs, an estimated K_d of ~150nM (Phe tRNA) and
239 ~130nM (mixed tRNA) was obtained (Figure 4B/C). In addition to EMSAs, Dbp5 binding to tRNA was
240 observed and tested in competition assays using fluorescence polarization measurements. In these
241 assays, increasing concentrations of unlabeled tRNA or a ssRNA homopolymeric polyadenylic acid (pA,
242 routinely used for RNA activation in steady-state ATPase assays (Weirich, Erzberger et al. 2006)), were
243 found to compete with a fluorescently labeled ssRNA for Dbp5 in the presence of ADP•BeF_3 (Figure 4D).
244 These data, from orthogonal approaches, indicate that Dbp5 interacts directly with tRNA *in vitro,* and
245 does so in a manner governed by principles that resemble Dbp5-ssRNA binding.

246 Interaction with ssRNA substrates has been well documented to stimulate the Dbp5 ATPase cycle
247 (Weirich, Erzberger et al. 2004, Lund and Guthrie 2005, Alcazar-Roman, Tran et al. 2006, Weirich,
248 Erzberger et al. 2006, Tran, Zhou et al. 2007, Dossani, Weirich et al. 2009, von Moeller, Basquin et al.
249 2009, Hodge, Tran et al. 2011, Montpetit, Thomsen et al. 2011, Noble, Tran et al. 2011). As such, it was
250 next determined if binding of tRNA to Dbp5 stimulates ATPase activity using a spectrophotometric
251 ATPase assay (Weirich, Erzberger et al. 2006, Montpetit, Thomsen et al. 2011). Unlike a ssRNA

252 substrate (i.e., pA) that can maximally stimulate ATP turnover to ~0.5 ATP/sec, neither tRNA nor poly(I:C)
253 (used as an orthogonal dsRNA substrate) stimulated Dbp5 ATPase activity over a range of RNA
254 concentrations (Figure 5A). These results with the above binding data suggest Dbp5 can engage
255 structured and dsRNA substrates, but this does not lead to productive ATP hydrolysis.

256 The nucleoporin Gle1 with the small molecule inositol hexakisphosphate ($InsP_6$) has been shown
257 to synergistically activate Dbp5 ATPase activity at low RNA concentrations (Weirich, Erzberger et al.
258 2006, Montpetit, Thomsen et al. 2011). These findings have led to a model of spatially regulated Dbp5
259 activity to promote mRNA-protein complex remodeling at the cytoplasmic face of an NPC where Gle1 is
260 localized, resulting in directional mRNA export (Hodge, Colot et al. 1999, Strahm, Fahrenkrog et al. 1999,
261 Alcazar-Roman, Tran et al. 2006, Weirich, Erzberger et al. 2006, Dossani, Weirich et al. 2009, Hodge,
262 Tran et al. 2011, Montpetit, Thomsen et al. 2011, Noble, Tran et al. 2011, Adams, Mason et al. 2017,
263 Wong, Gray et al. 2018, Arul Nambi Rajan and Montpetit 2021). In the context of tRNA, addition of
264 Gle1/$InsP_6$ maximally stimulated Dbp5 (1.03 +/- 0.04 ATP/s) to a level like that of ssRNA (1.11 +/- 0.07)
265 (Figure 5B). The synergistic activation of Dbp5 ATPase activity by Gle1/$InsP_6$ and tRNA is mirrored by
266 poly(I:C) and observed with both mixed yeast tRNAs as well as yeast Phenylalanine tRNA (Figure 5B).
267 To confirm that this enhanced RNA activation by Gle1/$InsP_6$ was not the result of contaminating ssRNA,
268 ATPase assays were performed after treatment of tRNA or poly (I:C) with RNase T1 for 2 hours at 37°C.
269 RNase T1 degrades ssRNA, not dsRNA, allowing determination of whether RNA activation observed in
270 the presence of Gle1/$InsP_6$ is specific to properly folded tRNA and poly(I:C). As expected, treatment of
271 the ssRNA (pA) with RNase T1 resulted in the loss of RNA-stimulated Dbp5 ATPase activity (0.68 +/-
272 0.06 before RNase T1 treatment to 0.17 +/- 0.01 after). Furthermore, RNase T1 treatment reduced
273 pA/Gle1/$InsP_6$ activation (0.98 +/- 0.17 before treatment to 0.69 +/-0.07 after) to that of Dbp5 and
274 Gle1/$InsP_6$ alone (0.62 +/- 0.03) (Figure 5C). However, RNase T1 treated tRNA remained unchanged in
275 the ability to activate Dbp5 in the presence of Gle1/$InsP_6$ (1.19+0.11 without vs 1.18+/-0.19 ATP/s with
276 RNase T1 treatment). This was recapitulated with poly(I:C) (1.26 +/- 0.11 ATP/s without and 1.46 +/-

277 0.135 ATP/s with RNase T1), confirming that the synergistic activation of Dbp5 observed in the presence
278 of Gle1/$InsP_6$ is dependent on the structured tRNA or dsRNA. These findings provide for the possibility
279 that Dbp5 engages tRNA in the cell without ATPase activation and could remain bound until the Dbp5-
280 tRNA complex reaches Gle1 at the cytoplasmic side of a nuclear pore complex.

281

282 **DISCUSSION**

283 The best characterized tRNA export factors in *S. cerevisiae*, Los1 and Msn5, are non-essential
284 and the *los1Δ/msn5Δ* double mutant is viable despite the essential role of tRNA export (Takano, Endo et
285 al. 2005, Murthi, Shaheen et al. 2010). These data suggest additional mechanisms for regulated tRNA
286 export, which is supported by recent publications that have implicated mRNA and rRNA export factors
287 such as Mex67, Nup159, Gle1, Dbp5, and Crm1 in tRNA export (Wu, Bao et al. 2015, Chatterjee,
288 Majumder et al. 2017, Nostramo and Hopper 2020, Chatterjee, Marshall et al. 2022). However, a
289 mechanistic understanding of how these factors function in tRNA export and how such roles differ or
290 relate to previously characterized roles in RNA export is still unresolved. Here, a combination of *in vivo*
291 and *in vitro* data provide evidence that (1) Dbp5 functions parallel to Los1 in tRNA export, similar to the
292 mRNA export factor Mex67 and Crm1; (2) Dbp5 can bind tRNA directly *in vitro* and does so independently
293 of Los1, Msn5, and Mex67 *in vivo*; and (3) the Dbp5 ATPase cycle is uniquely modulated by Gle1 in the
294 presence of structured RNA (e.g. tRNA or dsRNA) *in vitro* and the ATPase cycle supports tRNA export
295 *in vivo*.

296 Collectively, the *in vitro* characterization of Dbp5 and tRNA described here suggest two non-
297 mutually exclusive possibilities for why Dbp5 is only activated by tRNA/dsRNA in the presence of
298 Gle1/$InsP_6$. First, it may be that Dbp5 binds tRNA to form an inhibited intermediate that is relieved by
299 Gle1/$InsP_6$. This is an attractive hypothesis that is unique from how Dbp5 engages ssRNA (e.g., mRNA)
300 and potentially supports previously proposed export models that suggest Dbp5 may bind and travel with
301 a tRNA from nucleus to cytoplasm (Lari, Arul Nambi Rajan et al. 2019). A second possibility is that Gle1

302 enhances the affinity of Dbp5 for tRNA and “non-mRNA” substrates, which is supported by biochemical
303 characterizations that show Gle1 promotes a shift in the steady-state distribution of populated Dbp5
304 intermediates from weak to strong RNA binding states (Hodge, Tran et al. 2011, Montpetit, Thomsen et
305 al. 2011, Noble, Tran et al. 2011, Wong, Cao et al. 2016, Wong, Gray et al. 2018, Gray, Cao et al. 2022).
306 Future structural and biochemical studies are expected to distinguish among these possibilities.
307 Moreover, Dbp5 was previously reported to not bind dsRNA substrates (Weirich, Erzberger et al. 2006),
308 as such the findings that Dbp5 can bind, and in the presence of Gle1, be activated by tRNA should
309 motivate reevaluation of possible functions of Dbp5-Gle1/$InsP_6$ in regulating other highly structured RNA
310 or “non-canonical” substrates *in vivo*.

311 While it has been reported previously that tRNA fails to stimulate Dbp5 ATPase cycle (Tseng,
312 Weaver et al. 1998), here it is shown that despite a lack of stimulation when Gle1/$InsP_6$ is absent, Dbp5
313 is able to bind tRNA *in vitro* and *in vivo*. The ability of a tRNA to bind but not stimulate the ATPase cycle
314 of Dbp5 has important implications for mechanisms by which Dbp5 may function in tRNA export. For
315 example, in mRNA export it is thought that Dbp5 functions are localized at NPCs (Derrer, Mancini et al.
316 2019, Lari, Arul Nambi Rajan et al. 2019, Adams and Wente 2020), where the Dbp5 ATPase cycle is
317 tightly regulated by co-factors Nup159 and Gle1/$InsP_6$ (Hodge, Colot et al. 1999, Rollenhagen, Hodge et
318 al. 2004, Hodge, Tran et al. 2011, Montpetit, Thomsen et al. 2011, Noble, Tran et al. 2011, Wong, Gray
319 et al. 2018). In fact, recent studies have shown the essential function of both Dbp5 and Mex67 in mRNA
320 export can be accomplished when these proteins are fused to nuclear pore components, in addition Dbp5
321 does not form a complex with mRNAs in the nucleus (Derrer, Mancini et al. 2019, Adams and Wente
322 2020). These reports suggest that Dbp5 does not travel with an mRNA from the nucleoplasm to the
323 cytoplasmic face of an NPC as part of an mRNA-protein complex, rather Dbp5 likely engages mRNAs
324 after they exit the NPC transport channel to direct the final step(s) of mRNA export (Figure 6). However,
325 in contrast to this mRNA export model, the unique ability of Dbp5 to bind tRNA without ATP stimulation,
326 and then be fully activated by Gle1/$InsP_6$, presents the potential for a novel mechanism of function in

327 regulating tRNA export. Namely, that Dbp5 may enter the nucleus to stably engage tRNA and direct
328 events leading to export, following which Dbp5 is removed from the tRNA by Gle1/$InsP_6$ upon nuclear
329 exit (Figure 6). Importantly, in both mRNA and tRNA export, Gle1/$InsP_6$ activation is required to stimulate
330 ATPase activity and recycle the enzyme. In contrast, for pre-ribosomal subunit export Dbp5 ATPase
331 activity and Gle1 have been shown to be dispensable for transport (Neumann, Wu et al. 2016). This
332 raises interesting questions of whether RNA binding and nucleocytoplasmic shuttling of Dbp5 alone can
333 achieve this function, where in the cell these interactions occur, and how rRNA substrates modulate Dbp5
334 activity.

335 In mRNA export, it has been proposed that Dbp5 displaces mRNA export factors such as Mex67
336 and Nab2 to promote directionality of mRNA transit (Lund and Guthrie 2005, Tran, Zhou et al. 2007).
337 Observations that Mex67 and Dbp5 appear to both function parallel to Los1 to promote tRNA export may
338 point to an overlapping pathway that shares both mRNA export factors. Dbp5 and Mex67 have been
339 proposed to form physical interactions, with Mex67 serving as an adaptor to direct Dbp5 to appropriate
340 mRNA sites for remodeling (Lund and Guthrie 2005). However, here it is demonstrated that Mex67 is not
341 required for Dbp5-tRNA interaction based on RNA IP assays. Additionally, previously published data
342 suggests Mex67 likely requires an unknown adaptor to form its reported interactions with its tRNA
343 substrates (Yao, Roser et al. 2007). Given the *in vitro* properties of Dbp5 binding to tRNA, it is tempting
344 to speculate that nuclear Dbp5 promotes recruitment of Mex67 or Crm1 to tRNA-protein complexes.
345 Indeed, a similar phenomenon has been described for the exon junction complex (EJC) and the DEAD-
346 box protein at its core, eIF4AIII, that acts as a platform for the binding of other proteins to an mRNA
347 (Ballut, Marchadier et al. 2005, Andersen, Ballut et al. 2006, Bono, Ebert et al. 2006, Pacheco-Fiallos,
348 Vorlander et al. 2023). Stable binding of the EJC is governed by trans acting proteins that lock the
349 complex on the mRNA by stabilizing an ADP-P_i hydrolysis immediate (Ballut, Marchadier et al. 2005,
350 Bono, Ebert et al. 2006, Nielsen, Chamieh et al. 2009, Linder and Fuller-Pace 2013). In the case of Dbp5,
351 the *in vitro* data suggests an inhibited state may be achieved in the context of tRNA alone, which could

352 be further stabilized *in vivo* by yet to be discovered protein factors. The ability of Gle1/$InsP_6$ to induce
353 maximal activity of Dbp5 in the presence of tRNA would then allow for resolution of stable Dbp5-tRNA
354 complexes in a spatially regulated manner to terminate export and recycle bound export factors (Figure
355 6). Alternatively, given that it has been reported that Mex67 can bind 5´ extended tRNAs and that these
356 transcripts have been previously reported to contain 5´ methyl-guanosine cap structures (Ohira and
357 Suzuki 2016, Chatterjee, Marshall et al. 2022), perhaps an "mRNA export-like" pathway that involves
358 Cap Binding Complex (CBC) can act to recruit Mex67 to a subset of tRNAs. It remains unclear if CBC
359 interacts with such transcripts and whether other export factors like Dbp5 also support "premature" export
360 of unprocessed tRNAs.

361 More broadly, like many DEAD-box proteins, Dbp5 has many reported roles in controlling gene
362 expression (Estruch and Cole 2003, Rollenhagen, Hodge et al. 2004, Gross, Siepmann et al. 2007,
363 Scarcelli, Viggiano et al. 2008, Tieg and Krebber 2013, Wu, Becker et al. 2014, Neumann, Wu et al.
364 2016, Mikhailova, Shuvalova et al. 2017, Lari, Arul Nambi Rajan et al. 2019, Beissel, Grosse et al. 2020).
365 The nucleic acid substrate-specific biochemical properties of Dbp5 ATPase regulation defined here may
366 have wide-ranging implications for Dbp5 functions in pre-ribosomal RNA export, translation, or R-loop
367 metabolism. Furthermore, several DEAD-box proteins such as Dbp2 have been reported to bind diverse
368 nucleic acid substrates (ncRNA and mRNA), including G-Quadraplexes, and have roles in R-loop biology
369 (Ma, Paudel et al. 2016, Xing, Wang et al. 2017, Tedeschi, Cloutier et al. 2018, Gao, Byrd et al. 2019,
370 Lai, Choudhary et al. 2019, Lai and Tran 2021, Yan, Obi et al. 2021, Song, Lai et al. 2022). Given the
371 high degree of conservation in the structure, function, and regulation of Dbp5 with other DEAD-box
372 proteins (Ozgur, Buchwald et al. 2015, Sloan and Bohnsack 2018), the observations reported here raise
373 the possibility that other DEAD-box proteins may also have substrate-specific regulation.

374 Overall, this study and other recent publications support a general function for both Dbp5 and
375 Mex67 in RNA export (Yao, Roser et al. 2007, Yao, Lutzmann et al. 2008, Faza, Chang et al. 2012, Wu,
376 Becker et al. 2014, Neumann, Wu et al. 2016, Chatterjee, Majumder et al. 2017, Becker, Hirsch et al.

377 2019, Lari, Arul Nambi Rajan et al. 2019, Nostramo and Hopper 2020, Vasianovich, Bajon et al. 2020,
378 Chatterjee, Marshall et al. 2022). While these factors have been most well characterized in mRNA export,
379 it is now important to reconsider Dbp5 and Mex67 as general RNA export factors, which raises questions
380 about possible co-regulation of mRNA and non-coding RNA export pathways to fine tune gene
381 expression. To this end, the *in vitro*, biochemical, and genetic properties of Dbp5 reported in this study
382 will inform future structure-function and mechanistic characterization of a Dbp5 mediated, and Gle1
383 regulated, tRNA export pathway(s). For example, it will be important for future studies to address the
384 composition of pathway specific export-competent tRNA-protein complexes and how Dbp5 contributes
385 to changes in the architecture of such a complex as they move from nucleus to cytoplasm and back
386 again.

387 **MATERIALS AND METHODS**

388

389 **Yeast strains generation and growth conditions**

390 A list of all yeast strains used in this study is provided in Table S1. Deletion mutants and C-terminal
391 tagging was conducted by PCR based transformations and confirmed by colony PCR. All yeast
392 transformations were conducted using previously published standard high-efficiency LiAc, ssDNA, PEG
393 protocol (Gietz and Woods 2002). Yeast were cultured in YPD or synthetic complete (SC) media when
394 indicated to mid log growth. For overexpression of Dbp5 ATPase mutants, untagged Dbp5 or *dbp5*^{R426Q},
395 *dbp5*^{R369G}, or *dbp5*^{E240Q} were integrated at URA3 locus under control of pGAL promoter in a wild-type
396 strain with Dbp5 expressed from its endogenous locus and promoter. pGAL expression was induced by
397 first derepressing the promoter with growth in YP media with 2% raffinose overnight followed by a shift
398 to 2% galactose containing media for 6 hours. Overexpression was halted by addition of 2% glucose and
399 further incubation for 1 hour.

400

401 **Spot growth assay**

402 Yeast were pre-cultured to saturation overnight, diluted, and 1:10 serial dilutions were made with the
403 most concentrated wells representing a concentration of 0.25 OD/ml. 3 μL of each dilution was spotted
404 on YPD and grown at indicated temperatures for 2 days.

405

406 **Live Cell Imaging**

407 Imaging experiments were carried out using the confocal configuration of an Andor Dragonfly microscope
408 equipped with an EMCCD camera driven by Fusion software (Andor) using a 60x oil immersion objective
409 (Olympus, numerical aperture (N.A.) 1.4). Images were acquired from cells grown to mid log phase in SC
410 media at 25°C and shifted to 37°C for indicated time or treated with DMSO or 500uM Auxin and 10 uM

411 InsP6 for relevant experiments. Cells were immobilized in 384-well glass bottomed plates (VWR) that
412 were pre-treated with Concanavalin A.
413
414 **tRNA extraction and Northern Blotting**

415 Isolation of small RNAs and Northern blot experiments were performed as previously described (Wu,
416 Huang et al. 2013). Briefly, small RNAs were isolated from yeast cultures grown to early log phase by
417 addition of equal volumes cold TSE buffer (0.01M Tris pH7.5, 0.01M EDTA, 0.1M sodium chloride) and
418 TSE saturated phenol. Samples were incubated at 55°C for 20min with vortexing every 3 min then
419 placed on ice for 10 min. Aqueous phase was extracted after centrifugation, re-extraction with phenol
420 was performed, and RNA was precipitated overnight in ethanol at -80°C. 2.5ug of RNA was then
421 separated on 10% TBE-Urea gels, gels were stained with Apex safe DNA gel stain to visualize 25S and
422 18S rRNA and then transferred to Hybond N^+ membrane (Amersham). RNA was crosslinked to
423 membranes at 2400J/m^2 using UV Crosslinker (VWR) and tRNA were detected using digoxigenin-
424 labeled (DIG) probes. Mean integrated intensity values were measured for I and P bands using FIJI
425 (Schindelin, Arganda-Carreras et al. 2012) and normalized to background signal in each lane.

426 Sequence of Northern blot probe targeting precursor and mature isoforms of $tRNA^{Ile}_{UAU}$ used in Figure 2
427 and 4 is as follows:
428 GGCACAGAAACTTCGGAAACCGAATGTTGCTATAAGCACGAAGCTCTAACCACTGAGCTACACGA
429 GC.

430
431 **Fluorescence In-Situ Hybridization (FISH)**

432 FISH experiments were carried out as described in previous publications with minor modifications
433 (Lord, Ospovat et al. 2017) using directly Cy3 labeled tRNA probes or fluorescein isothiocyanate (FITC)

434 labeled dT probes. Sequence of Cy3 labeled $tRNA^{Ile}_{UAU}$ intron specific probe is same as previously
435 published SRIM03 (Chatterjee, Majumder et al. 2017) with Cy3 moiety appended at the 5´ end
436 (CGTTGCTTTTAAAGGCCTGTTTGAAAGGTCTTTGGCACAGAAACTTCGGAAACCGAATGTTGCTAT
437). Briefly, yeast cultures were grown to early log phase at 25°C and treated with drug/vehicle or shifted
438 to 37°C for 4 hours when appropriate. Samples were fixed with 0.1 volume of 37% formaldehyde for
439 15min. These samples were then pelleted and resuspended in 4% paraformaldehyde (PFA) solution
440 (4% PFA, 0.1M Potassium Phosphate (pH 6.5), 0.5mM $MgCl_2$) and incubated with rotation at 25°C for 3
441 hours. Cells were then washed twice with Buffer B (1.2M Sorbitol, 0.1M Potassium Phosphate (pH 6.5),
442 0.5mM $MgCl_2$). For spheroplasting cell pellets were resuspended in a 1ml Buffer B solution containing
443 0.05% beta-mercaptoethanol. 15ul of 20mg/mL zymolyase T20 was then added to each sample and
444 were subsequently incubated at 37°C for 45min. After washing once with Buffer B, cells were adhered
445 to eight well slides (Fisher Scientific) pre-coated with Poly-L-Lysine. Slides were placed sequentially in
446 70%, 90%, and 100% ethanol for 5min and then allowed to dry. Samples were next incubated at 37°C
447 for 2 hours in pre-hybridization buffer (4X SSC, 50% formamide, 10% dextran sulfate, 125 ug/mL *E. coli*
448 tRNA, 500 ug/mL salmon sperm DNA, 1x Denhardt's solution, and 10mM vanadyl ribonucleoside
449 complex (VRC)). Pre-hybridization solution was then aspirated and replaced with pre-warmed pre-
450 hybridization solution that contained either 0.25uM Cy3 tRNA probe or 0.025uM FITC dT probe and
451 further incubated at 37°C overnight. Wells were then sequentially washed for 5min once with 2x SSC,
452 three times with 1xSSC, and once with 0.5x SSC. Slides were dipped in 100% ethanol, air-dried, and
453 mounting media with 4', 6-diamidino-2-phenylidole (DAPI) was applied to each well prior to sealing of
454 coverslip onto slide. Imaging was performed using Andor Dragonfly equipped with Andor iXon Ultra 888
455 EMCCD camera driven by Fusion software (Andor) using a 60x 1.4 N.A. oil objective. Images were
456 processed in FIJI (e.g., cropping, brightness/contrast adjustments and maximum z-projections)
457 (Schindelin, Arganda-Carreras et al. 2012). Quantification of tRNA FISH was performed by acquiring
458 average nuclear and cytoplasmic pixel intensities respectively. Maximum projection images were
459 generated from z stack images for DAPI and tRNA FISH channels. Nuclear and whole cell masks were

460 then respectively generated using Cellpose software (Stringer, Wang et al. 2021, Pachitariu and
461 Stringer 2022). Nuclear mask regions were removed from whole cell masks to generate cytoplasmic
462 mask and average pixel intensities were calculated. The ratio of average nuclear and cytoplasmic mask
463 pixel intensity per cell was calculated.

464

465 **RNA Immunoprecipitation (RIP)**

466 RIPs were conducted as previously described with minor modifications (Lari, Arul Nambi Rajan et al.
467 2019). Pull downs were performed targeting protein-A (prA) tagged Dbp5 in parallel with an untagged
468 control to assess background non-specific binding. Crosslinking was conducted on yeast cultures in mid-
469 log growth by addition of formaldehyde to final concentration of 0.3% and incubation for 30 min.
470 Crosslinking was quenched by addition of glycine to a final concentration of 60mM for 10 min. Cells were
471 harvested and pellets frozen in liquid nitrogen. Lysis was performed using ice cold TN150 (50mM Tris-
472 HCl pH7.8, 150mM NaCl, 0.1% IGEPAL, 5mM beta-mercaptoethanol) supplemented with 10mM EDTA,
473 1ng Luciferase Spike-In RNA (Promega), and 1X protease inhibitor cocktail. 1ml zirconia beads (0.5mm)
474 were used for disrupting cells by vortexing 5 times for 30 seconds followed by 1min on ice between each
475 pulse. Lysate was pre-cleared by centrifugation at 4000xg 5min followed by 20min at 20000xg at 4°C.
476 1% pre-IP lysate was preserved as input RNA sample and additional pre-IP sample was reserved for
477 western blotting. Remaining lysates were then diluted to 10ml with TN150 and incubated with IgG-
478 conjugated magnetic dynabeads at 4°C for 30min with constant rotation. Immunoprecipitate was washed
479 once with 1ml TN150, once with 1ml TN1000 (50mM Tris-HCl pH7.8, 1M NaCl 0.1% IGEPAL, 5mM beta-
480 mercaptoethanol), and again once with 1ml TN150 each for 5min at 4°C. Beads from RIPs were then
481 resuspended in 500ul proteinase K elution mix (50mM Tris-HCl pH 7.8, 50mM NaCl, 1mM EDTA, 0.5%
482 SDS, 100ug proteinase K) in parallel with input samples and incubated at 50°C for 2 hours followed by
483 65°C for 1 hour to allow crosslink reversal. RNA was isolated by extraction with acidic
484 Phenol:Chloroform:Isoamylalcohol (pH 4.3-4.7) and ethanol precipitation. Half volume of RNA was

485 reverse transcribed using Superscript III using random priming according to manufacturer instructions
486 and other half of RNA was retained for minus RT control. RNA was analyzed by qPCR using Power
487 SYBR (Applied Biosystems) on an Applied Biosystems instrument. Target RNA abundance in RIP was
488 normalized to abundance of target in input sample and relative fold enrichment was calculated by
489 comparing signal in specific prA-Dbp5 RIPs to signal from untagged control. Standard curves were
490 generated to test PCR efficiencies of each primer set used in this study. Primer sequences used are as
491 follows:

492 $tRNA^{Ile}_{UAU}$ Unspliced Forward: GCTCGTGTAGCTCAGTGGTTAG

493 $tRNA^{Ile}_{UAU}$ Unspliced Reverse: CTTTTAAAGGCCTGTTTGAAAG

494 FBA1 Forward: CGAAAACGCTGACAAGGAAG

495 FBA1 Reverse: TCTCAAAGCGATGTCACCAG

496

497 **Western Blotting**

498 ~5 OD pellets were lysed in laemmli buffer and loaded onto 10% SDS PAGE. Protein transfer was
499 performed onto nitrocellulose membrane using cold wet tank transfer protocol. Western blotting was
500 performed with 1:5000 dilution of mouse monoclonal anti-DBP5 and 1:10000 dilution of mouse
501 monoclonal anti-GAPDH (Thermo Fisher) primary antibody overnight at 4°C and 1:10000 anti-mouse
502 DyeLight 650 secondary to detect protein.

503

504 **Protein Purification, ATPase assays and Fluorescence Polarization**

505 Protein purification, *in vitro* ATPase assays and fluorescence polarization using full-length Dbp5
506 performed as described previously (Weirich, Erzberger et al. 2006, Montpetit, Thomsen et al. 2011,
507 Montpetit, Seeliger et al. 2012). Commercially available Poly (I:C), mixed yeast tRNA and yeast
508 Phenylalanine tRNA were obtained from Sigma for use in indicated assays. For RNase T1 ATPase

509 assays, indicated RNA samples were treated with 33 units of RNase T1 for 2 hours at 37°C prior to
510 experiment. Fluorescence polarization experiments were performed using a fluorescein (fl) labelled 16nt
511 ssRNA (5'-fl-GGGUAAAAAAAAAAAA-3') in the presence of ADP•BeF_3 with increasing concentrations of
512 unlabeled polyadenylic acid or yeast mixed tRNA titrated into the reactions. Fluorescence polarization
513 and ATPase assays were assembled in the same ATPase buffer (30mM HEPES [pH 7.5], 100mM NaCl,
514 and 2mM $MgCl_2$). All ATPase assays with RNA titrations were fit to Michaelis Menten or allosteric
515 sigmoidal models (when Gle1/$InsP_6$ was added) in GraphPad Prism.

516

517 **RNA Electrophoretic Mobility Shift Assay (EMSA) and denaturing urea PAGE**

518 Recombinant full length Dbp5 was purified as above and described previously(Montpetit, Thomsen et al.
519 2011, Montpetit, Seeliger et al. 2012). RNA binding and EMSA was performed according to previously
520 published assay conditions (Yao, Roser et al. 2007). RNA binding reactions were assembled using
521 binding buffer (20mM HEPES [pH7.4], 100 mM KCl, 10 mM NaCl, 4 mM $MgCl_2$, 0.2 mM EDTA, 20%
522 glycerol, 1 mM DTT, 0.5% NP-40) in the presence of indicated nucleotide and loaded on to 6% native
523 polyacrylamide el (0.5 x TBE). Gels were stained with Apex gel stain to visualize RNA. Mean integrated
524 intensity of bands were quantified in FIJI (Schindelin, Arganda-Carreras et al. 2012) and normalized to
525 background signal for each respective well. Bound fraction was calculated and fit to a one-site binding
526 equation in GraphPad Prism.

527

528

ACKNOWLEDGEMENTS

We would like to acknowledge and thank all current and past members of the Montpetit lab for their aid and helpful discussions over the course of this work. Particularly we thank Rachel Montpetit for assistance with cloning and strain construction. We would also like to thank members of the Aitchison and Wozniak laboratories for their constructive feedback during this study. AANR was funded in part by the predoctoral Training Program in Molecular and Cellular Biology at UC Davis that is supported by an NIH T32 training grant (GM007377). RA was supported by a postdoctoral fellowship from Uehara memorial foundation and an overseas research fellowship from Japan Society for the Promotion of Science. Research was further supported by the National Institute of General Medical Sciences of the National Institutes of Health under Award Number R35GM145328. The content is solely the responsibility of the authors and does not necessarily represent the views of funding agencies.

542 **References**

543 Adams, R. L., A. C. Mason, L. Glass, Aditi and S. R. Wente (2017). "Nup42 and IP(6) coordinate Gle1
544 stimulation of Dbp5/DDX19B for mRNA export in yeast and human cells." Traffic **18**(12): 776-790.

545 Adams, R. L. and S. R. Wente (2020). "Dbp5 associates with RNA-bound Mex67 and Nab2 and its
546 localization at the nuclear pore complex is sufficient for mRNP export and cell viability." PLoS Genet
547 **16**(10): e1009033.

548 Alcazar-Roman, A. R., E. J. Tran, S. Guo and S. R. Wente (2006). "Inositol hexakisphosphate and Gle1
549 activate the DEAD-box protein Dbp5 for nuclear mRNA export." Nat Cell Biol **8**(7): 711-716.

550 Andersen, C. B., L. Ballut, J. S. Johansen, H. Chamieh, K. H. Nielsen, C. L. Oliveira, J. S. Pedersen, B.
551 Seraphin, H. Le Hir and G. R. Andersen (2006). "Structure of the exon junction core complex with a
552 trapped DEAD-box ATPase bound to RNA." Science **313**(5795): 1968-1972.

553 Arul Nambi Rajan, A. and B. Montpetit (2021). "Emerging molecular functions and novel roles for the
554 DEAD-box protein Dbp5/DDX19 in gene expression." Cell Mol Life Sci **78**(5): 2019-2030.

555 Bai, B., H. M. Moore and M. Laiho (2013). "CRM1 and its ribosome export adaptor NMD3 localize to the
556 nucleolus and affect rRNA synthesis." Nucleus **4**(4): 315-325.

557 Ballut, L., B. Marchadier, A. Baguet, C. Tomasetto, B. Seraphin and H. Le Hir (2005). "The exon junction
558 core complex is locked onto RNA by inhibition of eIF4AIII ATPase activity." Nat Struct Mol Biol **12**(10):
559 861-869.

560 Becker, D., A. G. Hirsch, L. Bender, T. Lingner, G. Salinas and H. Krebber (2019). "Nuclear Pre-snRNA
561 Export Is an Essential Quality Assurance Mechanism for Functional Spliceosomes." Cell Rep **27**(11):
562 3199-3214 e3193.

563 Beissel, C., S. Grosse and H. Krebber (2020). "Dbp5/DDX19 between Translational Readthrough and
564 Nonsense Mediated Decay." Int J Mol Sci **21**(3).

565 Bono, F., J. Ebert, E. Lorentzen and E. Conti (2006). "The crystal structure of the exon junction complex
566 reveals how it maintains a stable grip on mRNA." Cell **126**(4): 713-725.

567 Chatterjee, K., S. Majumder, Y. Wan, V. Shah, J. Wu, H. Y. Huang and A. K. Hopper (2017). "Sharing the
568 load: Mex67-Mtr2 cofunctions with Los1 in primary tRNA nuclear export." Genes Dev **31**(21): 2186-
569 2198.

570 Chatterjee, K., W. A. Marshall and A. K. Hopper (2022). "Three tRNA nuclear exporters in S. cerevisiae:
571 parallel pathways, preferences, and precision." Nucleic Acids Res **50**(17): 10140-10152.

572 Cook, A. G., N. Fukuhara, M. Jinek and E. Conti (2009). "Structures of the tRNA export factor in the
573 nuclear and cytosolic states." Nature **461**(7260): 60-65.

574 Derrer, C. P., R. Mancini, P. Vallotton, S. Huet, K. Weis and E. Dultz (2019). "The RNA export factor
575 Mex67 functions as a mobile nucleoporin." J Cell Biol **218**(12): 3967-3976.

576 Dossani, Z. Y., C. S. Weirich, J. P. Erzberger, J. M. Berger and K. Weis (2009). "Structure of the C-
577 terminus of the mRNA export factor Dbp5 reveals the interaction surface for the ATPase activator
578 Gle1." Proc Natl Acad Sci U S A **106**(38): 16251-16256.

579 Estruch, F. and C. N. Cole (2003). "An early function during transcription for the yeast mRNA export
580 factor Dbp5p/Rat8p suggested by its genetic and physical interactions with transcription factor IIH
581 components." Mol Biol Cell **14**(4): 1664-1676.

582 Eswara, M. B., A. T. McGuire, J. B. Pierce and D. Mangroo (2009). "Utp9p facilitates Msn5p-mediated
583 nuclear reexport of retrograded tRNAs in Saccharomyces cerevisiae." Mol Biol Cell **20**(23): 5007-5025.

584 Fan, J. S., Z. Cheng, J. Zhang, C. Noble, Z. Zhou, H. Song and D. Yang (2009). "Solution and crystal
585 structures of mRNA exporter Dbp5p and its interaction with nucleotides." J Mol Biol **388**(1): 1-10.

586 Faza, M. B., Y. Chang, L. Occhipinti, S. Kemmler and V. G. Panse (2012). "Role of Mex67-Mtr2 in the
587 nuclear export of 40S pre-ribosomes." PLoS Genet **8**(8): e1002915.

588 Feng, W. and A. K. Hopper (2002). "A Los1p-independent pathway for nuclear export of intronless
589 tRNAs in Saccharomycescerevisiae." Proc Natl Acad Sci U S A **99**(8): 5412-5417.

590 Gao, J., A. K. Byrd, B. L. Zybailov, J. C. Marecki, M. J. Guderyon, A. D. Edwards, S. Chib, K. L. West, Z. J.
591 Waldrip, S. G. Mackintosh, Z. Gao, A. A. Putnam, E. Jankowsky and K. D. Raney (2019). "DEAD-box RNA
592 helicases Dbp2, Ded1 and Mss116 bind to G-quadruplex nucleic acids and destabilize G-quadruplex
593 RNA." Chem Commun (Camb) **55**(31): 4467-4470.

594 Gietz, R. D. and R. A. Woods (2002). "Transformation of yeast by lithium acetate/single-stranded
595 carrier DNA/polyethylene glycol method." Methods Enzymol **350**: 87-96.

596 Graczyk, D., M. Ciesla and M. Boguta (2018). "Regulation of tRNA synthesis by the general transcription
597 factors of RNA polymerase III - TFIIIB and TFIIIC, and by the MAF1 protein." Biochim Biophys Acta Gene
598 Regul Mech **1861**(4): 320-329.

599 Gray, S., W. Cao, B. Montpetit and E. M. De La Cruz (2022). "The nucleoporin Gle1 activates DEAD-box
600 protein 5 (Dbp5) by promoting ATP binding and accelerating rate limiting phosphate release." Nucleic
601 Acids Res **50**(7): 3998-4011.

602 Gross, T., A. Siepmann, D. Sturm, M. Windgassen, J. J. Scarcelli, M. Seedorf, C. N. Cole and H. Krebber
603 (2007). "The DEAD-box RNA helicase Dbp5 functions in translation termination." Science **315**(5812):
604 646-649.

605 Guerrier-Takada, C., K. Gardiner, T. Marsh, N. Pace and S. Altman (1983). "The RNA moiety of
606 ribonuclease P is the catalytic subunit of the enzyme." Cell **35**(3 Pt 2): 849-857.

607 Harris, M. E. (2016). "Theme and Variation in tRNA 5' End Processing Enzymes: Comparative Analysis of
608 Protein versus Ribonucleoprotein RNase P." J Mol Biol **428**(1): 5-9.

609 Haruki, H., J. Nishikawa and U. K. Laemmli (2008). "The anchor-away technique: rapid, conditional
610 establishment of yeast mutant phenotypes." Mol Cell **31**(6): 925-932.

611 Hodge, C. A., H. V. Colot, P. Stafford and C. N. Cole (1999). "Rat8p/Dbp5p is a shuttling transport factor
612 that interacts with Rat7p/Nup159p and Gle1p and suppresses the mRNA export defect of xpo1-1 cells."
613 EMBO J **18**(20): 5778-5788.

614 Hodge, C. A., E. J. Tran, K. N. Noble, A. R. Alcazar-Roman, R. Ben-Yishay, J. J. Scarcelli, A. W. Folkmann,
615 Y. Shav-Tal, S. R. Wente and C. N. Cole (2011). "The Dbp5 cycle at the nuclear pore complex during
616 mRNA export I: dbp5 mutants with defects in RNA binding and ATP hydrolysis define key steps for
617 Nup159 and Gle1." Genes Dev **25**(10): 1052-1064.

618 Hopper, A. K. and H. Y. Huang (2015). "Quality Control Pathways for Nucleus-Encoded Eukaryotic tRNA
619 Biosynthesis and Subcellular Trafficking." Mol Cell Biol **35**(12): 2052-2058.

620 Huang, H. Y. and A. K. Hopper (2015). "In vivo biochemical analyses reveal distinct roles of beta-
621 importins and eEF1A in tRNA subcellular traffic." Genes Dev **29**(7): 772-783.

622 Jankowsky, E. (2011). "RNA helicases at work: binding and rearranging." Trends Biochem Sci **36**(1): 19-
623 29.

624 Kaminski, T., J. P. Siebrasse and U. Kubitscheck (2013). "A single molecule view on Dbp5 and mRNA at
625 the nuclear pore." Nucleus **4**(1): 8-13.

626 Lai, Y. H., K. Choudhary, S. C. Cloutier, Z. Xing, S. Aviran and E. J. Tran (2019). "Genome-Wide Discovery
627 of DEAD-Box RNA Helicase Targets Reveals RNA Structural Remodeling in Transcription Termination."
628 Genetics **212**(1): 153-174.

629 Lai, Y. H. and E. J. Tran (2021). "Probing Transcriptome-Wide RNA Structural Changes Dependent on
630 the DEAD-box Helicase Dbp2." Methods Mol Biol **2209**: 287-305.

631 Lari, A., A. Arul Nambi Rajan, R. Sandhu, T. Reiter, R. Montpetit, B. P. Young, C. J. Loewen and B.
632 Montpetit (2019). "A nuclear role for the DEAD-box protein Dbp5 in tRNA export." Elife **8**.

633 Linder, P. and F. V. Fuller-Pace (2013). "Looking back on the birth of DEAD-box RNA helicases." Biochim
634 Biophys Acta **1829**(8): 750-755.

635 Lord, C. L., O. Ospovat and S. R. Wente (2017). "Nup100 regulates Saccharomyces cerevisiae replicative
636 life span by mediating the nuclear export of specific tRNAs." RNA **23**(3): 365-377.

637 Lund, M. K. and C. Guthrie (2005). "The DEAD-box protein Dbp5p is required to dissociate Mex67p
638 from exported mRNPs at the nuclear rim." Mol Cell **20**(4): 645-651.

639 Ma, W. K., B. P. Paudel, Z. Xing, I. G. Sabath, D. Rueda and E. J. Tran (2016). "Recruitment, Duplex
640 Unwinding and Protein-Mediated Inhibition of the Dead-Box RNA Helicase Dbp2 at Actively Transcribed
641 Chromatin." J Mol Biol **428**(6): 1091-1106.

642 Mason, A. C. and S. R. Wente (2020). "Functions of Gle1 are governed by two distinct modes of self-
643 association." J Biol Chem **295**(49): 16813-16825.

644 Mikhailova, T., E. Shuvalova, A. Ivanov, D. Susorov, A. Shuvalov, P. M. Kolosov and E. Alkalaeva (2017).
645 "RNA helicase DDX19 stabilizes ribosomal elongation and termination complexes." Nucleic Acids Res
646 **45**(3): 1307-1318.

647 Montpetit, B., M. A. Seeliger and K. Weis (2012). "Analysis of DEAD-box proteins in mRNA export."
648 Methods Enzymol **511**: 239-254.

649 Montpetit, B., N. D. Thomsen, K. J. Helmke, M. A. Seeliger, J. M. Berger and K. Weis (2011). "A
650 conserved mechanism of DEAD-box ATPase activation by nucleoporins and InsP6 in mRNA export."
651 Nature **472**(7342): 238-242.

652 Murthi, A., H. H. Shaheen, H. Y. Huang, M. A. Preston, T. P. Lai, E. M. Phizicky and A. K. Hopper (2010).
653 "Regulation of tRNA bidirectional nuclear-cytoplasmic trafficking in Saccharomyces cerevisiae." Mol
654 Biol Cell **21**(4): 639-649.

655 Neumann, B., H. Wu, A. Hackmann and H. Krebber (2016). "Nuclear Export of Pre-Ribosomal Subunits
656 Requires Dbp5, but Not as an RNA-Helicase as for mRNA Export." PLoS One **11**(2): e0149571.

657 Nielsen, K. H., H. Chamieh, C. B. Andersen, F. Fredslund, K. Hamborg, H. Le Hir and G. R. Andersen
658 (2009). "Mechanism of ATP turnover inhibition in the EJC." RNA **15**(1): 67-75.

659 Nishimura, K., T. Fukagawa, H. Takisawa, T. Kakimoto and M. Kanemaki (2009). "An auxin-based degron
660 system for the rapid depletion of proteins in nonplant cells." Nat Methods **6**(12): 917-922.

661 Noble, K. N., E. J. Tran, A. R. Alcazar-Roman, C. A. Hodge, C. N. Cole and S. R. Wente (2011). "The Dbp5
662 cycle at the nuclear pore complex during mRNA export II: nucleotide cycling and mRNP remodeling by
663 Dbp5 are controlled by Nup159 and Gle1." Genes Dev **25**(10): 1065-1077.

664 Nostramo, R. T. and A. K. Hopper (2020). "A novel assay provides insight into tRNAPhe retrograde
665 nuclear import and re-export in S. cerevisiae." Nucleic Acids Res **48**(20): 11577-11588.

666 Ohira, T. and T. Suzuki (2016). "Precursors of tRNAs are stabilized by methylguanosine cap structures."
667 Nat Chem Biol **12**(8): 648-655.

668 Ozgur, S., G. Buchwald, S. Falk, S. Chakrabarti, J. R. Prabu and E. Conti (2015). "The conformational
669 plasticity of eukaryotic RNA-dependent ATPases." FEBS J **282**(5): 850-863.

670 Pacheco-Fiallos, B., M. K. Vorlander, D. Riabov-Bassat, L. Fin, F. J. O'Reilly, F. I. Ayala, U. Schellhaas, J.
671 Rappsilber and C. Plaschka (2023). "mRNA recognition and packaging by the human transcription-
672 export complex." Nature **616**(7958): 828-835.

673 Pachitariu, M. and C. Stringer (2022). "Cellpose 2.0: how to train your own model." Nat Methods
674 **19**(12): 1634-1641.

675 Phizicky, E. M. and A. K. Hopper (2023). "The Life and Times of a tRNA." RNA.

676 Rollenhagen, C., C. A. Hodge and C. N. Cole (2004). "The nuclear pore complex and the DEAD box
677 protein Rat8p/Dbp5p have nonessential features which appear to facilitate mRNA export following
678 heat shock." Mol Cell Biol **24**(11): 4869-4879.

679 Scarcelli, J. J., S. Viggiano, C. A. Hodge, C. V. Heath, D. C. Amberg and C. N. Cole (2008). "Synthetic
680 genetic array analysis in Saccharomyces cerevisiae provides evidence for an interaction between
681 RAT8/DBP5 and genes encoding P-body components." Genetics **179**(4): 1945-1955.

682 Schindelin, J., I. Arganda-Carreras, E. Frise, V. Kaynig, M. Longair, T. Pietzsch, S. Preibisch, C. Rueden, S.
683 Saalfeld, B. Schmid, J. Y. Tinevez, D. J. White, V. Hartenstein, K. Eliceiri, P. Tomancak and A. Cardona
684 (2012). "Fiji: an open-source platform for biological-image analysis." Nat Methods **9**(7): 676-682.

685 Schmitt, C., C. von Kobbe, A. Bachi, N. Pante, J. P. Rodrigues, C. Boscheron, G. Rigaut, M. Wilm, B.
686 Seraphin, M. Carmo-Fonseca and E. Izaurralde (1999). "Dbp5, a DEAD-box protein required for mRNA
687 export, is recruited to the cytoplasmic fibrils of nuclear pore complex via a conserved interaction with
688 CAN/Nup159p." EMBO J **18**(15): 4332-4347.

689 Sengoku, T., O. Nureki, A. Nakamura, S. Kobayashi and S. Yokoyama (2006). "Structural basis for RNA
690 unwinding by the DEAD-box protein Drosophila Vasa." Cell **125**(2): 287-300.

691 Shi, H. and P. B. Moore (2000). "The crystal structure of yeast phenylalanine tRNA at 1.93 A resolution:
692 a classic structure revisited." RNA **6**(8): 1091-1105.

693 Skowronek, E., P. Grzechnik, B. Spath, A. Marchfelder and J. Kufel (2014). "tRNA 3' processing in yeast
694 involves tRNase Z, Rex1, and Rrp6." RNA **20**(1): 115-130.

695 Sloan, K. E. and M. T. Bohnsack (2018). "Unravelling the Mechanisms of RNA Helicase Regulation."
696 Trends Biochem Sci **43**(4): 237-250.

697 Snay-Hodge, C. A., H. V. Colot, A. L. Goldstein and C. N. Cole (1998). "Dbp5p/Rat8p is a yeast nuclear
698 pore-associated DEAD-box protein essential for RNA export." EMBO J **17**(9): 2663-2676.

699 Song, Q. X., C. W. Lai, N. N. Liu, X. M. Hou and X. G. Xi (2022). "DEAD-box RNA helicase Dbp2 binds to G-
700 quadruplex nucleic acids and regulates different conformation of G-quadruplex DNA." Biochem
701 Biophys Res Commun **634**: 182-188.

702 Steiner-Mosonyi, M., D. M. Leslie, H. Dehghani, J. D. Aitchison and D. Mangroo (2003). "Utp8p is an
703 essential intranuclear component of the nuclear tRNA export machinery of Saccharomyces cerevisiae."
704 J Biol Chem **278**(34): 32236-32245.

705 Strahm, Y., B. Fahrenkrog, D. Zenklusen, E. Rychner, J. Kantor, M. Rosbach and F. Stutz (1999). "The
706 RNA export factor Gle1p is located on the cytoplasmic fibrils of the NPC and physically interacts with

707 the FG-nucleoporin Rip1p, the DEAD-box protein Rat8p/Dbp5p and a new protein Ymr 255p." EMBO J
708 **18**(20): 5761-5777.

709 Stringer, C., T. Wang, M. Michaelos and M. Pachitariu (2021). "Cellpose: a generalist algorithm for
710 cellular segmentation." Nat Methods **18**(1): 100-106.

711 Takano, A., T. Endo and T. Yoshihisa (2005). "tRNA actively shuttles between the nucleus and cytosol in
712 yeast." Science **309**(5731): 140-142.

713 Takemura, R., Y. Inoue and S. Izawa (2004). "Stress response in yeast mRNA export factor: reversible
714 changes in Rat8p localization are caused by ethanol stress but not heat shock." J Cell Sci **117**(Pt 18):
715 4189-4197.

716 Tedeschi, F. A., S. C. Cloutier, E. J. Tran and E. Jankowsky (2018). "The DEAD-box protein Dbp2p is
717 linked to noncoding RNAs, the helicase Sen1p, and R-loops." RNA **24**(12): 1693-1705.

718 Thoms, M., E. Thomson, J. Bassler, M. Gnadig, S. Griesel and E. Hurt (2015). "The Exosome Is Recruited
719 to RNA Substrates through Specific Adaptor Proteins." Cell **162**(5): 1029-1038.

720 Tieg, B. and H. Krebber (2013). "Dbp5 - from nuclear export to translation." Biochim Biophys Acta
721 **1829**(8): 791-798.

722 Tran, E. J., Y. Zhou, A. H. Corbett and S. R. Wente (2007). "The DEAD-box protein Dbp5 controls mRNA
723 export by triggering specific RNA:protein remodeling events." Mol Cell **28**(5): 850-859.

724 Trotta, C. R., F. Miao, E. A. Arn, S. W. Stevens, C. K. Ho, R. Rauhut and J. N. Abelson (1997). "The yeast
725 tRNA splicing endonuclease: a tetrameric enzyme with two active site subunits homologous to the
726 archaeal tRNA endonucleases." Cell **89**(6): 849-858.

727 Tseng, S. S., P. L. Weaver, Y. Liu, M. Hitomi, A. M. Tartakoff and T. H. Chang (1998). "Dbp5p, a cytosolic
728 RNA helicase, is required for poly(A)+ RNA export." EMBO J **17**(9): 2651-2662.

729 Tudek, A., M. Schmid, M. Makaras, J. D. Barrass, J. D. Beggs and T. H. Jensen (2018). "A Nuclear Export
730 Block Triggers the Decay of Newly Synthesized Polyadenylated RNA." Cell Rep **24**(9): 2457-2467 e2457.

731 Vasianovich, Y., E. Bajon and R. J. Wellinger (2020). "Telomerase biogenesis requires a novel Mex67
732 function and a cytoplasmic association with the Sm(7) complex." Elife **9**.

733 von Moeller, H., C. Basquin and E. Conti (2009). "The mRNA export protein DBP5 binds RNA and the
734 cytoplasmic nucleoporin NUP214 in a mutually exclusive manner." Nat Struct Mol Biol **16**(3): 247-254.

735 Wan, Y. and A. K. Hopper (2018). "From powerhouse to processing plant: conserved roles of
736 mitochondrial outer membrane proteins in tRNA splicing." Genes Dev **32**(19-20): 1309-1314.

737 Weirich, C. S., J. P. Erzberger, J. M. Berger and K. Weis (2004). "The N-terminal domain of Nup159
738 forms a beta-propeller that functions in mRNA export by tethering the helicase Dbp5 to the nuclear
739 pore." Mol Cell **16**(5): 749-760.

740 Weirich, C. S., J. P. Erzberger, J. S. Flick, J. M. Berger, J. Thorner and K. Weis (2006). "Activation of the
741 DExD/H-box protein Dbp5 by the nuclear-pore protein Gle1 and its coactivator InsP6 is required for
742 mRNA export." Nat Cell Biol **8**(7): 668-676.

743 Wong, E. V., W. Cao, J. Voros, M. Merchant, Y. Modis, D. D. Hackney, B. Montpetit and E. M. De La Cruz
744 (2016). "P(I) Release Limits the Intrinsic and RNA-Stimulated ATPase Cycles of DEAD-Box Protein 5
745 (Dbp5)." J Mol Biol **428**(2 Pt B): 492-508.

746 Wong, E. V., S. Gray, W. Cao, R. Montpetit, B. Montpetit and E. M. De La Cruz (2018). "Nup159
747 Weakens Gle1 Binding to Dbp5 But Does Not Accelerate ADP Release." J Mol Biol **430**(14): 2080-2095.

748 Wu, H., D. Becker and H. Krebber (2014). "Telomerase RNA TLC1 shuttling to the cytoplasm requires
749 mRNA export factors and is important for telomere maintenance." Cell Rep **8**(6): 1630-1638.

750 Wu, J., A. Bao, K. Chatterjee, Y. Wan and A. K. Hopper (2015). "Genome-wide screen uncovers novel
751 pathways for tRNA processing and nuclear-cytoplasmic dynamics." Genes Dev **29**(24): 2633-2644.

752 Wu, J. and A. K. Hopper (2014). "Healing for destruction: tRNA intron degradation in yeast is a two-step
753 cytoplasmic process catalyzed by tRNA ligase Rlg1 and 5'-to-3' exonuclease Xrn1." Genes Dev **28**(14):
754 1556-1561.

755 Wu, J., H. Y. Huang and A. K. Hopper (2013). "A rapid and sensitive non-radioactive method applicable
756 for genome-wide analysis of Saccharomyces cerevisiae genes involved in small RNA biology." Yeast
757 **30**(4): 119-128.

758 Xing, Z., S. Wang and E. J. Tran (2017). "Characterization of the mammalian DEAD-box protein DDX5
759 reveals functional conservation with S. cerevisiae ortholog Dbp2 in transcriptional control and glucose
760 metabolism." RNA **23**(7): 1125-1138.

761 Yan, K. K., I. Obi and N. Sabouri (2021). "The RGG domain in the C-terminus of the DEAD box helicases
762 Dbp2 and Ded1 is necessary for G-quadruplex destabilization." Nucleic Acids Res **49**(14): 8339-8354.

763 Yao, W., M. Lutzmann and E. Hurt (2008). "A versatile interaction platform on the Mex67-Mtr2
764 receptor creates an overlap between mRNA and ribosome export." EMBO J **27**(1): 6-16.

765 Yao, W., D. Roser, A. Kohler, B. Bradatsch, J. Bassler and E. Hurt (2007). "Nuclear export of ribosomal
766 60S subunits by the general mRNA export receptor Mex67-Mtr2." Mol Cell **26**(1): 51-62.

767 Yoshihisa, T., C. Ohshima, K. Yunoki-Esaki and T. Endo (2007). "Cytoplasmic splicing of tRNA in
768 Saccharomyces cerevisiae." Genes Cells **12**(3): 285-297.

769 Yoshihisa, T., K. Yunoki-Esaki, C. Ohshima, N. Tanaka and T. Endo (2003). "Possibility of cytoplasmic pre-
770 tRNA splicing: the yeast tRNA splicing endonuclease mainly localizes on the mitochondria." Mol Biol
771 Cell **14**(8): 3266-3279.

772 Zhao, J., S. B. Jin, B. Bjorkroth, L. Wieslander and B. Daneholt (2002). "The mRNA export factor Dbp5 is
773 associated with Balbiani ring mRNP from gene to cytoplasm." EMBO J **21**(5): 1177-1187.

774

775

776

777

778

779 **Figure Legends**

780 ***Figure 1: Dbp5 functions parallel to Los1 in pre-tRNA$^{Ile}_{UAU}$ export***

781 (A) Fluorescent images show GFP-Dbp5 remains enriched at the nuclear periphery in wild-type and
782 *los1Δ* at 25°C and 37°C. Scale bar represents 2 µm.

783 (B) Los1-GFP remains nucleoplasmic and associated with nuclear periphery in Dbp5-AID after treatment
784 with DMSO or 500 µM Auxin and 10 µM $InsP_6$ for 90 minutes. Scale bar represents 2 µm.

785 (C) dT FISH confirms induction of mRNA export defect and Dbp5 loss of function after addition of 500
786 µM Auxin and 10 µM $InsP_6$ in Dbp5-AID strain for 90 minutes. Scale bar represents 2 µm.

787 (D) Spot assay for growth of strains containing untagged *dbp5^{L12A}, dbp5^{R423A},* or *los1Δ* integrated at the
788 endogenous gene locus after two days at 25, 30, and 37°C on YPD.

789 (E) tRNA FISH targeting intron of tRNA$^{Ile}_{UAU}$ in indicated strains after pre-culture to early log phase at
790 25°C and shift to 37°C for 4 hours. Scale bar represents 2 µm.

791 (F) Quantification of tRNA FISH from (E). Ratio of average nuclear to cytoplasmic pixel intensities were
792 calculated across 3 independent replicate experiments and pooled for plotting. P-values were
793 calculated using one-way ANOVA.

794 (G) Northern Blot analysis targeting precursor and mature isoforms of tRNA$^{Ile}_{UAU}$. Small RNAs were
795 isolated from strains at mid log phase growth after pre-culture at 25°C and shift to 37°C for 4 hours.

796 (H) Quantification of Northern blot from (G). Ratio of signal from intron-containing end processed
797 intermediates (I) vs 5' leader/3' trailer containing precursor (P) was calculated and presented relative
798 to I/P ratio observed for WT. Error bars represent standard deviation and p-values calculated using
799 one-way ANOVA.

800

801 ***Figure 2: Los1 and Mex67 are not required for Dbp5 recruitment to pre-tRNA$^{Ile}_{UAU}$***

802 (A) Plots show relative fold enrichment of tRNA$^{Ile}_{UAU}$ following prA-Dbp5 RNA IP in a wild-type (WT),
803 *los1Δ,* and *msn5Δ* strain background. Abundance of target gene is normalized to abundance of the

804 target transcript in input samples and represented as fold enrichment relative to RNA IP from an
805 untagged control.
806 (B) prA-Dbp5 RNA IP targeting $tRNA^{Ile}_{UAU}$ in Mex67-AA after either treatment with DMSO or 1 μg/ml
807 rapamycin for 15 minutes.
808 (C) prA-Dbp5 RNA IP targeting FBA1 mRNA in Mex67-AA after either treatment with DMSO or 1 μg/ml
809 rapamycin for 15 minutes.
810 (D) dT FISH confirming a mRNA export defect caused by loss of function of Mex67 following 15min
811 incubation with 1 μg/ml rapamycin compared to a DMSO control. Scale bar represents 2 μm.
812
813 ***Figure 3: ATPase activity and Gle1 is required for Dbp5-mediated tRNA export in vivo***
814 (A) Western blot with either mouse monoclonal anti-DBP5 or anti-GAPDH (loading control) antibody to
815 detect overexpression of untagged Dbp5 and Dbp5 ATPase mutants. Strains were cultured in
816 raffinose at 25°C to derepress pGAL promoter and expression was induced by shifting cultures into
817 2% galactose containing media for 6 hours. Expression was stopped by addition of glucose for 1
818 hour. Overexpression was observed over the level of wildtype Dbp5 that is expressed from the
819 endogenous locus and is present in the pre-induction samples. Top and bottom panels are from the
820 same blot and processed equally.
821 (B) dT FISH confirms previously reported mRNA export status phenotypes for Dbp5 ATPase mutants
822 with $dbp5^{R426Q}$ and $dbp5^{R369G}$ showing a nuclear accumulation of poly(A)-RNA. Scale bar represents
823 2 μm.
824 (C) Northern blot analysis targeting precursor and mature isoforms of $tRNA^{Ile}_{UAU}$ from yeast strains
825 overexpressing *DBP5*, $dbp5^{R426Q}$, $dbp5^{R369G}$, or $dbp5^{E240Q}$.
826 (D) Quantification of Northern blot from (C). Ratio of signal from intron-containing end processed
827 intermediates (I) vs 5' leader/3' trailer containing precursor (P) was calculated and presented relative

828 to I/P ratio observed for WT. Error bars represent standard deviation and p-values calculated using
829 one-way ANOVA.
830
831 ***Figure 4: Dbp5 binds yeast tRNA in vitro***
832 (A) Full length recombinant Dbp5 (fl-Dbp5) binds both mixed yeast tRNA and Phenylalanine (Phe) tRNA
833 in the presence of the ATP mimetic ADP•BeF_3 by electrophoresis mobility shift assay (EMSA). RNA
834 binding reaction was conducted in the presence of ADP•BeF_3, ATP, ADP, or no nucleotide and
835 resolved on 6% native polyacrylamide gel at 70V. Reactions contained 2 μM fl-Dbp5, 1 mM nucleotide
836 when present, 250ng tRNA and binding buffer.
837 (B) EMSA experiments in which increasing concentrations of fl-Dbp5 was titrated into RNA binding
838 reactions in the presence of 1 mM ADP•BeF_3, 250ng mixed yeast tRNA or Phe tRNA, and binding
839 buffer.
840 (C) Band intensities of free probe and band shifts were quantified, and bound fraction was calculated for
841 each well of EMSAs in (B). One site binding model was fit to the data using GraphPad Prism to
842 estimate Kd for both mixed yeast tRNA and Phe tRNA.
843 (D) Unlabeled pA ssRNA and mixed yeast tRNA compete with a 16nt fluorescein labelled ssRNA for fl-
844 Dbp5 binding. Fluorescence polarization competition assays were performed by titrating increasing
845 concentration of an unlabeled competitor, pA (open square) or mixed yeast tRNA (closed circle), in
846 reactions containing 50 nM fluorescein labelled ssRNA, 2.5 mM ADP•BeF_3, 1 μM Dbp5 and buffer.
847 Error bars represent standard deviation of three independent experiments.
848
849 ***Figure 5: tRNA alone does not stimulate the Dbp5 ATPase cycle but can act synergistically with***
850 ***Gle1/InsP$_6$ to fully activate Dbp5***
851 (A) ATPase activity of Dbp5 is stimulated by ssRNA (pA, closed square) but not mixed yeast tRNA
852 (closed diamond), Phe tRNA (open square), or poly (I:C) dsRNA (open circle). Steady-state ATPase
853 assays were conducted in the presence of 1 μM Dbp5, 2.5 mM ATP, and varying concentrations of

854 RNA. Data was fit to Michaelis-Menten equation using GraphPad Prism. Error bars represent
855 standard deviation of three independent experiments.
856 (B) Gle1/$InsP_6$ synergistically stimulates Dbp5 ATPase activity with mixed yeast tRNA (closed diamond),
857 Phe tRNA (open square) and poly (I:C) dsRNA (open circle) substrates like ssRNA (pA). Steady-state
858 ATPase assays were conducted in presence of 1 μM Dbp5, 2.5 mM ATP, 2 μM Gle1, 2 μM $InsP_6$,
859 and varying concentration of RNA. Data was fit to an allosteric sigmoidal model in GraphPad Prism.
860 Error bars represent standard deviation of three independent experiments.
861 (C) RNase T1 treatment of RNA for 2 hours at 37°C prior to ATPase assays confirms that the observed
862 synergistic activation of Dbp5 ATPase activity by Gle1/$InsP_6$ and tRNA or dsRNA is not caused by
863 low levels of contaminating ssRNA. Steady-state ATPase assays were conducted in presence of 1
864 μM Dbp5, 2.5 mM ATP, 0.2 mg/ml RNA and 2 μM Gle1/$InsP_6$ when indicated.
865

866 **Figure 6: Model of Dbp5 function in mRNA, tRNA and pre-ribosomal subunit export**

867 Data from this study support a model in which Dbp5-mediated export of both mRNA and tRNA require
868 Gle1/$InsP_6$ activation to remodel RNPs at the cytoplasmic face of the Nuclear Pore Complex. For tRNA
869 export, lack of RNA-mediated ATPase stimulation following RNA binding may lead to formation of tRNA
870 bound intermediates that act as adapters for recruitment of yet to be identified transport factors. For
871 mRNA export, it has been shown that Dbp5 function is limited to the nuclear periphery and Dbp5 does
872 not form stable nuclear complexes with mRNA. Gle1/$InsP_6$ mediated activation of Dbp5 catalytic cycle
873 and RNA release likely promotes recycling of export factors and Dbp5 to function in further rounds of
874 export or other functions. In contrast, for Dbp5 mediated pre-ribosomal subunit export Dbp5 ATPase
875 cycle and Gle1/$InsP_6$ stimulation are dispensable for transport. As such, RNA binding may promote export
876 through an unknown mechanism and that Dbp5-mediated remodeling does not occur at NPCs, with
877 factors such as Mex67 persisting on pre-ribosomal subunits following export to the cytoplasm.

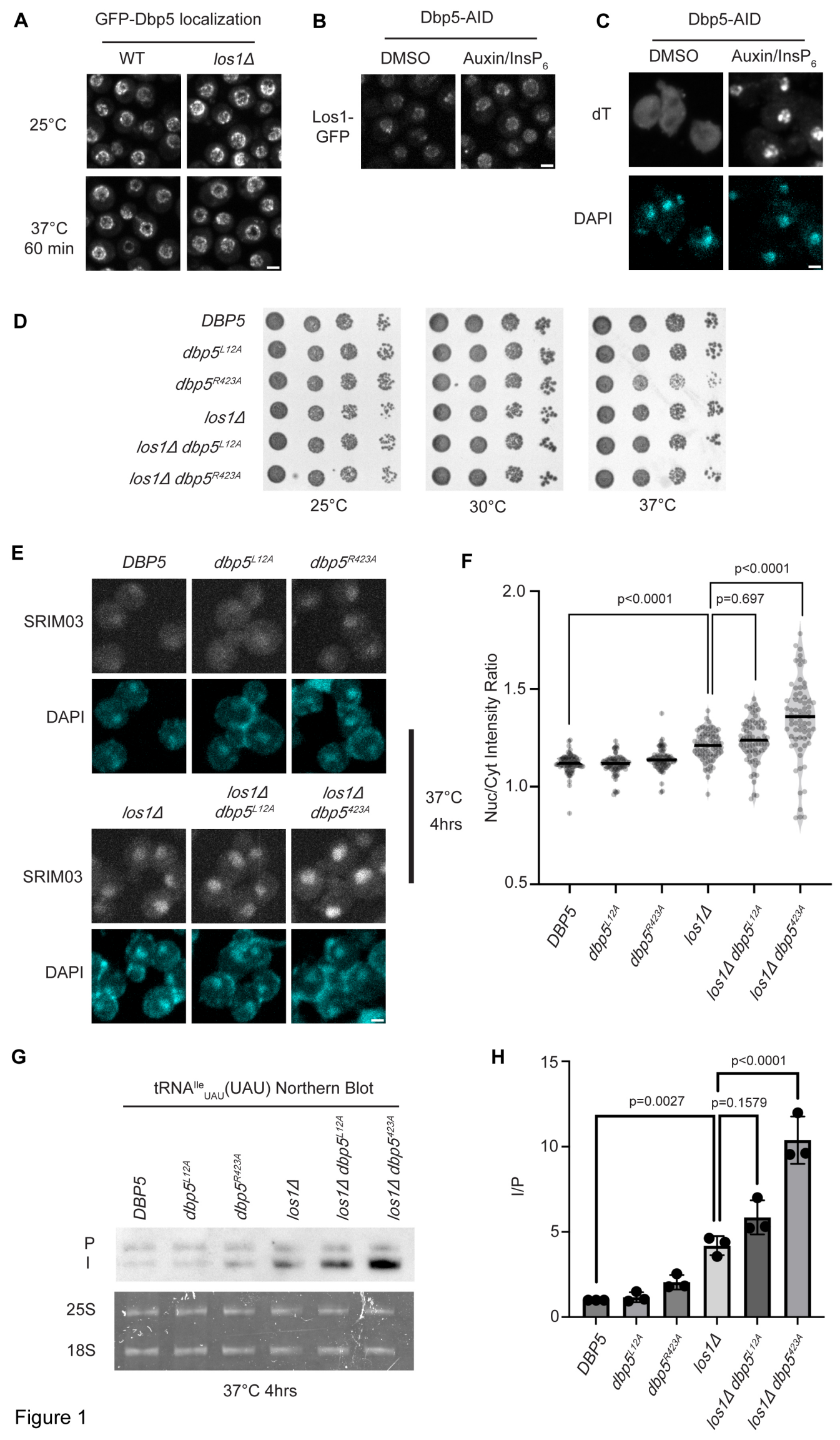
A
GFP-Dbp5 localization
WT
los1Δ
25°C
37°C
60 min
B
Dbp5-AID
DMSO
Auxin/InsP6
Los1-GFP
C
Dbp5-AID
DMSO
Auxin/InsP6
dT
DAPI
D
DBP5
dbp5L12A
dbp5R423A
los1Δ
los1Δ dbp5L12A
los1Δ dbp5R423A
25°C
30°C
37°C
E
DBP5
dbp5L12A
dbp5R423A
SRIM03
DAPI
los1Δ
los1Δ dbp5L12A
los1Δ dbp5423A
SRIM03
DAPI
37°C
4hrs
F
p<0.0001
p<0.0001
p=0.697
Nuc/Cyt Intensity Ratio
2.0
1.5
1.0
0.5
DBP5
dbp5L12A
dbp5R423A
los1Δ
los1Δ dbp5L12A
los1Δ dbp5423A
G
tRNAIleUAU(UAU) Northern Blot
DBP5
dbp5L12A
dbp5R423A
los1Δ
los1Δ dbp5L12A
los1Δ dbp5423A
P
I
25S
18S
37°C 4hrs
H
p<0.0001
p=0.0027
p=0.1579
I/P
15
10
5
0
DBP5
dbp5L12A
dbp5R423A
los1Δ
los1Δ dbp5L12A
los1Δ dbp5423A

Figure 1

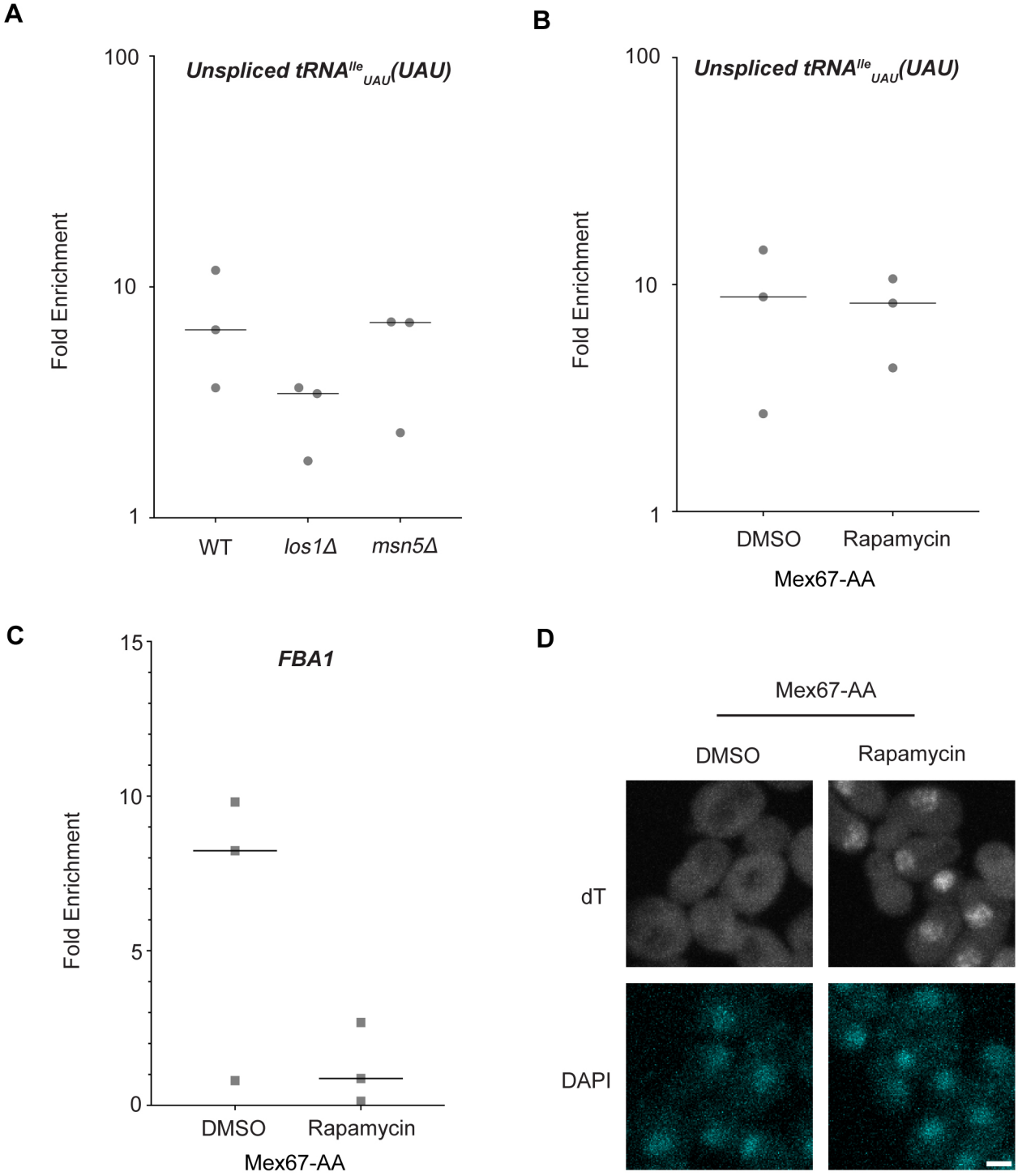
A
Unspliced tRNA$^{Ile}_{UAU}$(UAU)
Fold Enrichment
100
10
1
WT
los1Δ
msn5Δ
B
Unspliced tRNA$^{Ile}_{UAU}$(UAU)
Fold Enrichment
100
10
1
DMSO
Rapamycin
Mex67-AA
C
FBA1
Fold Enrichment
15
10
5
0
DMSO
Rapamycin
Mex67-AA
D
Mex67-AA
DMSO
Rapamycin
dT
DAPI

Figure 2

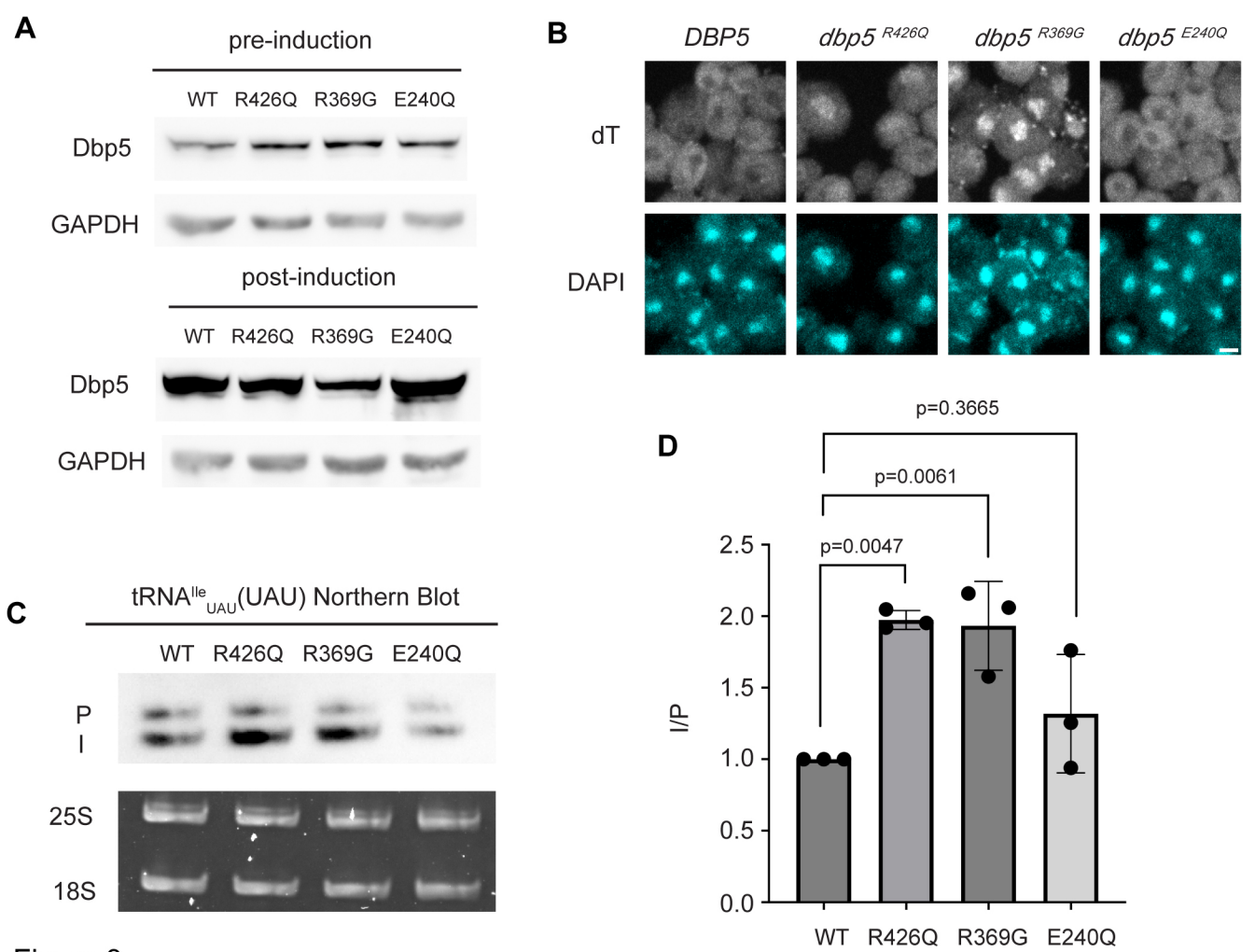
A
pre-induction
WT R426Q R369G E240Q
Dbp5
GAPDH
post-induction
WT R426Q R369G E240Q
Dbp5
GAPDH
B
DBP5
dbp5 R426Q
dbp5 R369G
dbp5 E240Q
dT
DAPI
C
tRNA Ile UAU (UAU) Northern Blot
WT R426Q R369G E240Q
P
I
25S
18S
D
p=0.3665
p=0.0061
p=0.0047
I/P
2.5
2.0
1.5
1.0
0.5
0.0
WT R426Q R369G E240Q

Figure 3

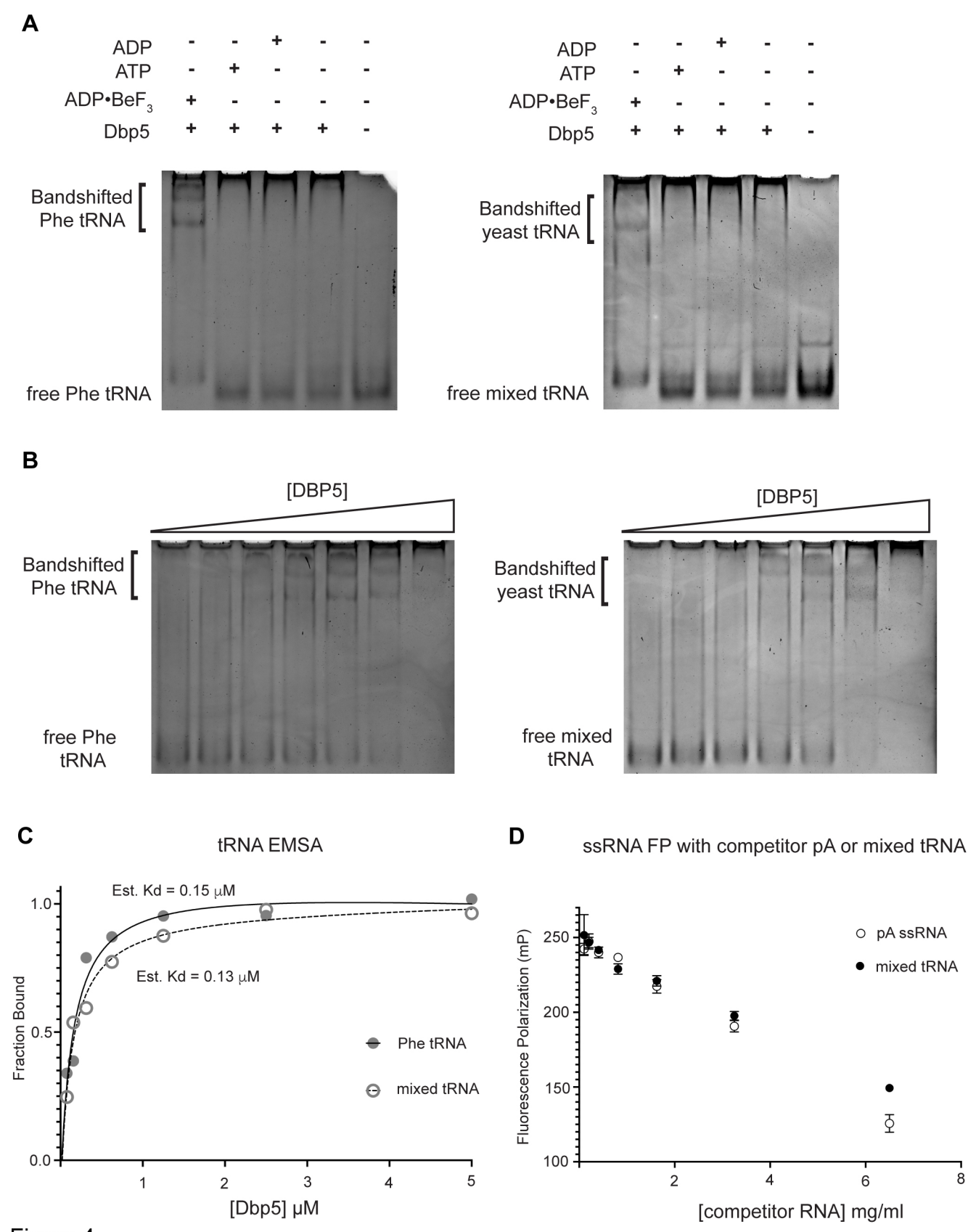
A
ADP - - + - -
ATP - + - - -
ADP•BeF3 + - - - -
Dbp5 + + + + -
Bandshifted Phe tRNA
free Phe tRNA
ADP - - + - -
ATP - + - - -
ADP•BeF3 + - - - -
Dbp5 + + + + -
Bandshifted yeast tRNA
free mixed tRNA
B
[DBP5]
Bandshifted Phe tRNA
free Phe tRNA
[DBP5]
Bandshifted yeast tRNA
free mixed tRNA
C
tRNA EMSA
Est. Kd = 0.15 μM
Est. Kd = 0.13 μM
Fraction Bound
1.0
0.5
0.0
1
2
3
4
5
[Dbp5] μM
Phe tRNA
mixed tRNA
D
ssRNA FP with competitor pA or mixed tRNA
Fluorescence Polarization (mP)
250
200
150
100
2
4
6
8
[competitor RNA] mg/ml
pA ssRNA
mixed tRNA

Figure 4

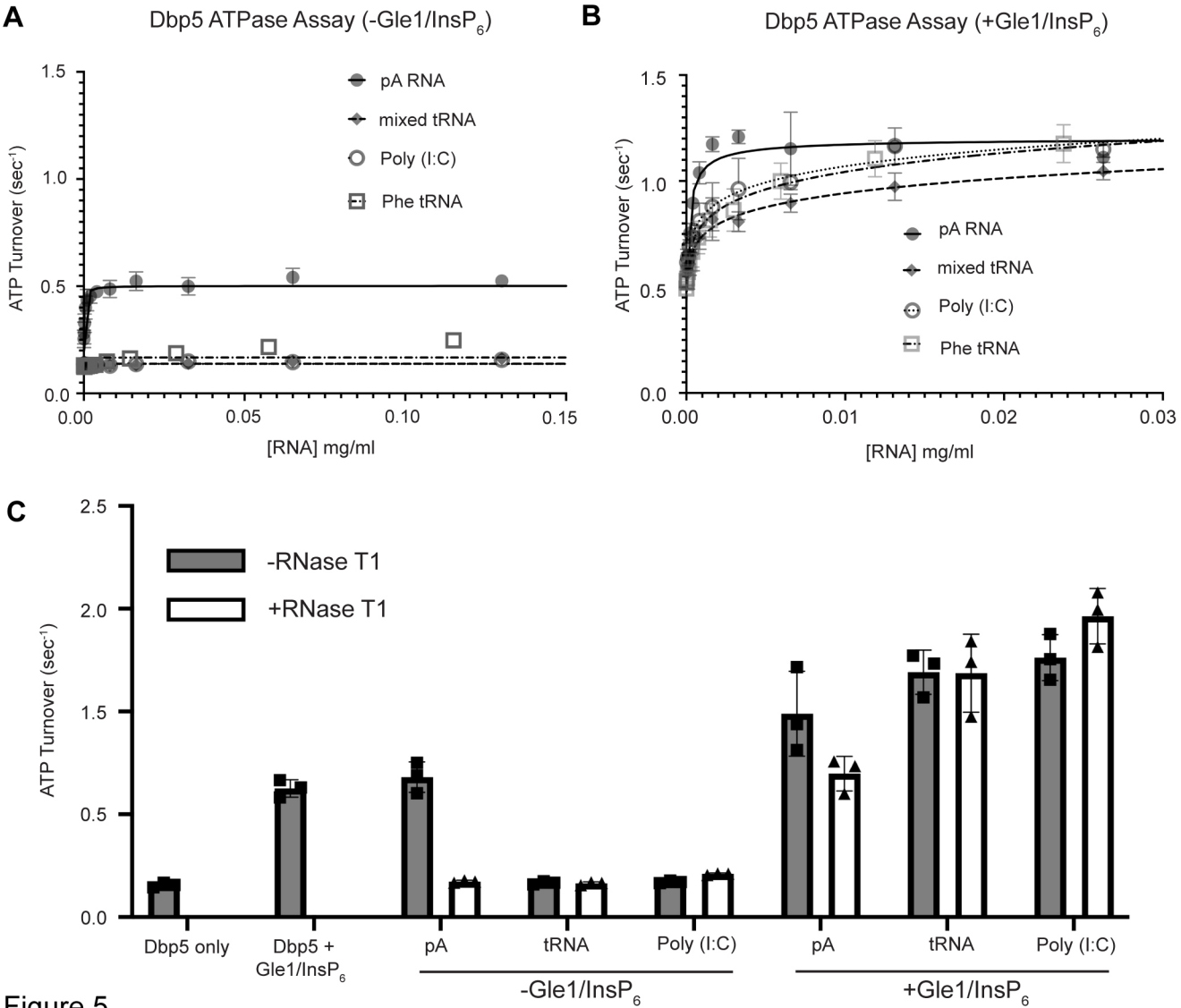
A
Dbp5 ATPase Assay (-Gle1/InsP6)
ATP Turnover (sec-1)
[RNA] mg/ml
pA RNA
mixed tRNA
Poly (I:C)
Phe tRNA
B
Dbp5 ATPase Assay (+Gle1/InsP6)
ATP Turnover (sec-1)
[RNA] mg/ml
pA RNA
mixed tRNA
Poly (I:C)
Phe tRNA
C
ATP Turnover (sec-1)
-RNase T1
+RNase T1
Dbp5 only
Dbp5 + Gle1/InsP6
pA
tRNA
Poly (I:C)
-Gle1/InsP6
pA
tRNA
Poly (I:C)
+Gle1/InsP6

Figure 5

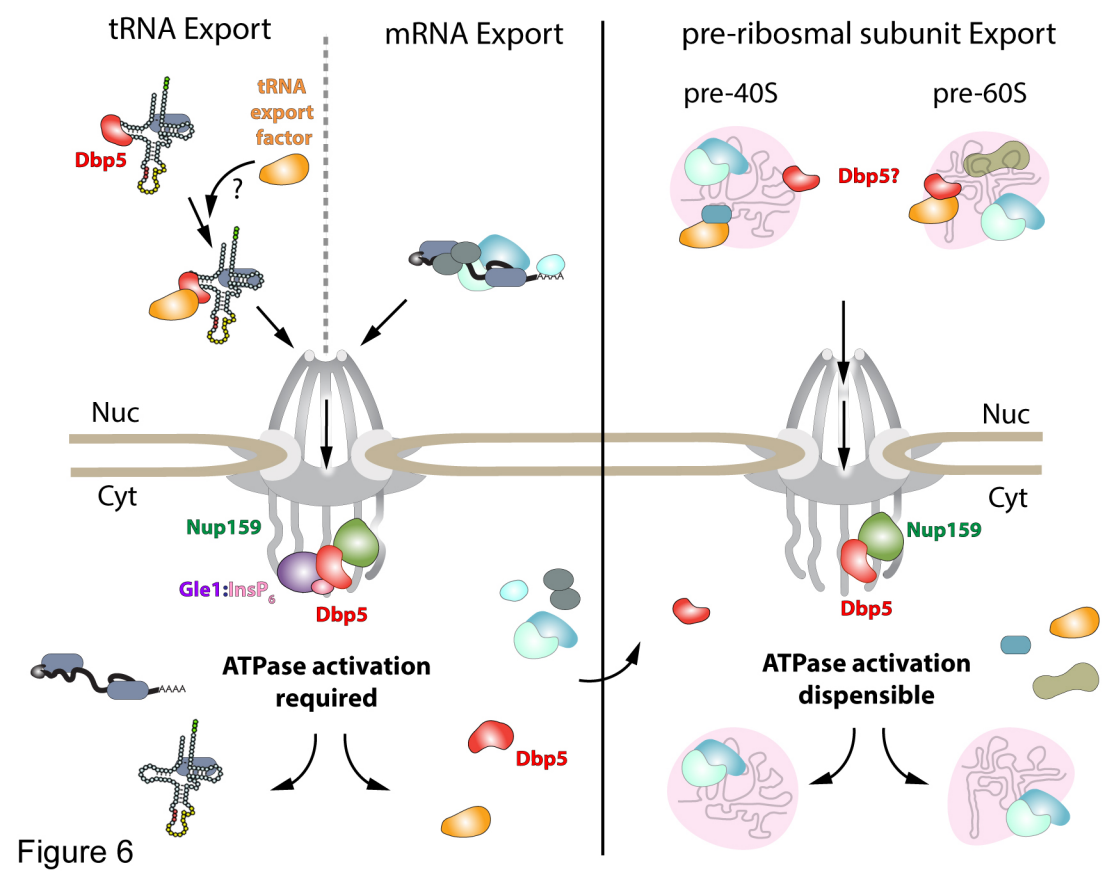
tRNA Export
mRNA Export
pre-ribosmal subunit Export
tRNA export factor
Dbp5
?
pre-40S
pre-60S
Dbp5?
Nuc
Cyt
Nup159
Gle1:InsP6
Dbp5
AAAA
ATPase activation required
ATPase activation dispensible

Figure 6